ISSN (print): 1698-6180. ISSN (online): 1886-7995
www.ucm.es/info/estratig/journal.htm

Journal of Iberian Geology 34 (2) 2008: 191-213

Journal of Iberian Geology
AN INTERNATIONAL PUBLICATION OF EARTH SCIENCES

Modern conditions and recent environmental development of the Muskiz estuary: historical disturbance by the largest oil refinery of Spain

Caracterización actual y evolución ambiental reciente de la Ría de Muskiz: impacto histórico de la mayor refinería de petróleo de España

A. Cearreta[1], M. Alday[2], M. J. Irabien[3], N. Etxebarria[4], J. Soto[5]

[1]Departamento de Estratigrafía y Paleontología, Facultad de Ciencia y Tecnología, Universidad del País Vasco/E.H.U., Apartado 644, 48080 Bilbao, Spain. E-mail: alejandro.cearreta@ehu.es
[2]Departamento de Geologia, Faculdade de Ciências, Universidade de Lisboa, Bloco C6, Campo Grande, 1749-016 Lisboa, Portugal
[3]Departamento de Mineralogía y Petrología, Facultad de Ciencia y Tecnología, Universidad del País Vasco/E.H.U., Apartado 644, 48080 Bilbao, Spain
[4]Departamento de Química Analítica, Facultad de Ciencia y Tecnología, Universidad del País Vasco/E.H.U., Apartado 644, 48080 Bilbao, Spain.
[5]Departamento de Ciencias Médicas y Quirúrgicas, Facultad de Medicina, Universidad de Cantabria, Avda. Cardenal Herrera Oria s/n, 39011 Santander, Spain

Received: 02/05/07 / Accepted: 13/09/07

Abstract

In 1970 the largest oil refinery in Spain was built on the Muskiz estuary and occupies most of its original surface. An integrated high-resolution microfaunal-geochemical study has revealed the evolution and environmental development of this estuary during the last 120 years, mainly by the identification and assessment of natural processes versus anthropogenic impacts. Benthic foraminifera, trace elements and PAHs data from surface sediment samples and sediment cores from the meagre remaining intertidal flat and marsh areas together with short-life radiometric isotope determinations provide a chronology for environmental changes in this estuary. Concentrations of organic and inorganic pollutant, both in modern and recent materials, are generally low and show no significative variations in space or time, except those associated to sedimentological changes in the core records. Natural processes in the middle estuary indicate the change from previous sandy, normal-salinity conditions to a muddy brackish environment around 1914. Anthropogenic impacts are not related to persistent historical pollution on this estuary but merely to the occupation of the estuary and the elimination of its different original ecosystems, so causing a general impoverishment of its environmental quality.

Keywords: benthic foraminifera, trace elements, PAHs, ^{137}Cs and ^{210}Pb dating, sedimentary record, anthropogenic impact, Muskiz estuary

Resumen

En 1970 se construyó en la Ría de Muskiz la mayor refinería de petróleo de España ocupando la mayor parte de los dominios estuarinos originales. Este trabajo utiliza un enfoque integrado geoquímico-micropaleontológico de alta resolución con el fin de examinar la evolución estuarina y el desarrollo ambiental de esta zona costera durante los últimos 120 años, distinguiendo particularmente entre los procesos naturales e impactos antrópicos. Se analizaron foraminíferos bentónicos, elementos traza e hidrocarburos

aromáticos policíclicos a partir de muestras superficiales y testigos sedimentarios recogidos de las escasas llanuras intermareales y zonas de marisma. También se llevaron a cabo determinaciones de isótopos radiométricos de vida corta con el fin de obtener una cronología para las variaciones ambientales detectadas en este estuario. Las concentraciones de contaminantes orgánicos e inorgánicos, tanto en los materiales actuales como históricos, son generalmente bajas y no muestran variaciones espaciales o temporales significativas, excepto las que aparecen asociadas a cambios sedimentológicos en los testigos. Los procesos naturales en la zona media del estuario indican una variación desde unas condiciones previas de carácter arenoso y salinidad marino normal hasta un medio fangoso y salobre alrededor de 1914. El impacto humano no parece relacionado con una persistente contaminación histórica en este estuario sino más bien con la extensiva ocupación del medio estuarino que destruyó sus ecosistemas originales para asentar la refinería de petróleo, provocando así un empobrecimiento generalizado de su calidad ambiental.

Palabras clave: foraminíferos bentónicos, elementos traza, PAHs, datación ^{137}Cs y ^{210}Pb, registro sedimentario, impacto humano, Ría de Muskiz.

1. Introduction

The Muskiz estuary, on the northern coast of Spain, forms the tidal part of the Barbadun River and originally occupied 204 Ha. The main channel has been modified and isolated by the construction of dykes from its original intertidal areas, and nowadays it has a length of 5,6 km and an average width of between 5-10 m. The only remains of the original estuarine environments are located in the lower estuary, with a dune field on the right bank (total surface area 10,4 Ha) and some marsh areas on the left bank (total surface area 15 Ha) (Fig. 1). It is a mesotidal estuary with semidiurnal tides ranging from 4,96 m during spring tides to less than 1,7 m during neaps. The estuary is partially mixed and the average input of fresh water is approximately 3 m^3 s^{-1} (Gobierno Vasco, 1998a, b).

The first human exploitation of the area commenced in 6,000 yr BP (Zapata, 1995) and Roman and Medieval settlements have been found in the original estuarine domain (Apellaniz and Nolte, 1967). During the last 125 years, the natural features of the Muzkiz estuary have been modified dramatically, initially by the reclamation of marshes for agriculture which now occupy 66% of the original estuarine domain. The increasing exploitation of the local iron ore in the inland parts of the fluvial valley since the 16th century has led to the outpouring of abundant mining waste into the estuary. In 1970 the largest oil refinery in Spain, with a processing capacity of 11 million tons $year^{-1}$, was built in the estuary and occupies 75% of its original area (including the previous reclaimed areas; Fig. 1) (Rivas, 1991).

The modern channel can be divided into three sections based on sediment grain size: the upper estuary, with low contents of gravel (average 4%) and equal amounts of muddy and sandy sediment; the middle estuary dominated by muddy sediment (average 60%); and the lower estuary dominated by sandy sediments (average 100%) (Gobierno Vasco, 1999). The muddy middle estuary area receives waste from two sources: the oil refinery (5 million m^3 yr^{-1}) and a wastewater treatment plant opened in 1988 (almost 1 million m^3 yr^{-1}) (Gobierno Vasco, 1998b). The highest contents of organic matter in the sediments (7-9%) occur around these waste disposal points (Gobierno Vasco, 1999).

This study uses an integrated high-resolution microfaunal-geochemical approach to examine the evolution and environmental development of the Muskiz estuary during the last century. One of the main aims of this work is the identification and assessment of natural versus anthropogenic processes in this area. Benthic foraminifera, trace elements and PAHs data from surface sediments and sediment cores collected from intertidal flat and marsh areas are presented. ^{210}Pb and ^{137}Cs determinations have also been undertaken to provide a chronology of the environmental changes in this estuary.

2. Materials and methods

Surface sediment samples were collected for micropalaeontological analysis from 17 sites in the tidal flats close to the estuarine channel and 27 sites in the marsh area during October-December 2000 (Fig. 1). Samples for geochemical analysis were taken from the same sites and at the same time as those for the micropalaeontological study, whereas the samples for PAHs analysis in the estuarine intertidal flats (1-16) were taken in February 2003. Five additional micropalaeontological samples were taken from the middle estuary (samples 8-12) for comparative purposes only in September 2001. Sampling sites close to the main channel were selected where exposure of intertidal flats allowed collection at regular distances. In the marsh area samples were collected along 7 transects (named A to G) in order to cover different subenvironments. Surface samples consist mainly of brown and black sandy muds and muddy sands.

Two sediment cores (Cores B and M), 50 cm in length, were also collected from the middle estuarine intertidal mudflat in September 2001 and the marsh in November 2003 respectively (Fig. 1). Two PVC tubes (12.5 cm di-

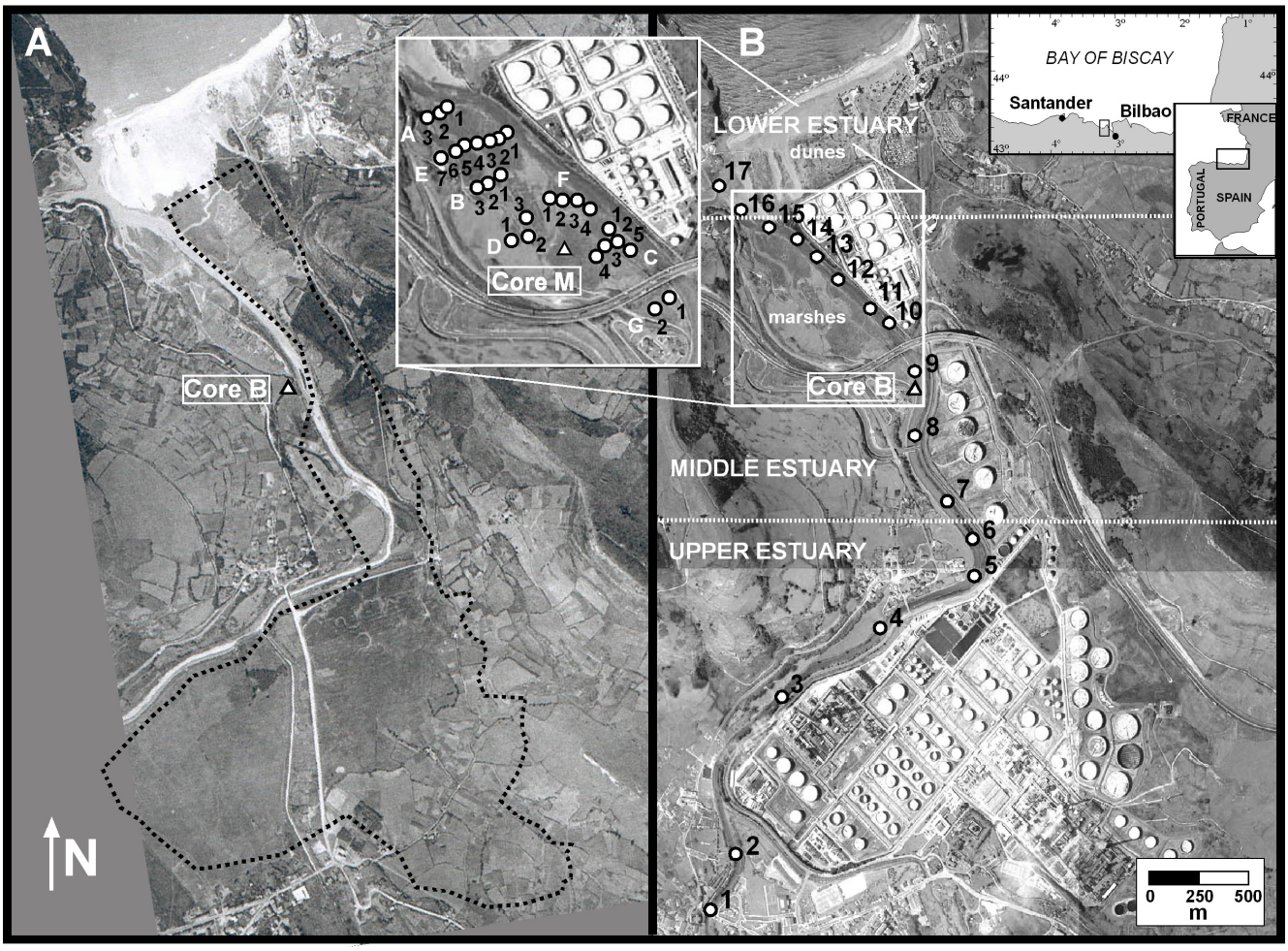

Fig. 1.- Geographic location of the Muskiz estuary, showing the position of the surface samples (dots) and short cores (triangles) in the intertidal flat and marsh areas. A: Aerial photograph showing the estuary in 1965 and the future emplacement of the refinery; B: Aerial photograph showing the estuary in 1999.

Fig.1.- Localización geográfica de la Ría de Muskiz, mostrando la posición de las muestras superficiales (puntos) y los pequeños sondeos (triángulos) en las zonas de canal y marisma. A: fotografía aérea del estuario en 1965; B: fotografía aéra del estuario en 1999.

ameter) were inserted into the sediment at each sampling location in order to obtain sufficient material to determine the benthic foraminifera, trace elements, PAHs content, organic matter (Core M only) and ^{137}Cs and ^{210}Pb geochronologies. Compaction of the sediment during sampling was negligible. Cores were described, photographed and X-radiographed before being sliced into succesive 1-cm samples. Furthermore, deeper sediments were sampled down to 1 m depth by means of a Russian sampler (Eijkelkamp peat sampler) at the Core B location and the results integrated with those from the PVC tube samples.

2.1. Microfaunal study

A hard plastic ring was pressed into the surface layer and the top 1-2 cm of oxygenated sediment was placed in a bottle containing ethanol. This process was repeated twice to sample a total of 80 cm^3 of sediment. Samples were sieved through 1 mm (to exclude large organic fragments) and 63-micron sieves and washed to remove clay and silt grade material. When clean, the contents remaining on the sieve (ie the sand grade material) were added to an equal volume of Rose Bengal and left for an hour following Walton's (1952) method. Rose Bengal stains protoplasm bright red and therefore stained forms, presumed to be alive at the time of collection, could be easily differentiated from unstained empty tests (dead individuals). The sample was sieved and washed to remove the excess stain and then dried at 50 ^{o}C. Foraminifera were concentrated by flotation in trichlorethylene as described by Murray (1979). Where possible, tests were picked until a representative amount of more than 300 individuals was obtained. Otherwise, all the available tests were picked and studied under a stereoscopic binocular microscope using reflected light. Altogether, 49 samples and

more than 30,000 foraminifera were examined from the surface sediments. All foraminiferal species identified in these samples are listed in Appendix 1.

Core samples were analyzed for foraminiferal content at 1-cm intervals following the same procedure as described for the surface samples, except that they were not stained. In total, 74 samples and more than 16,000 foraminifera were studied from the core samples. All foraminiferal species identified in the core samples are also listed in Appendix 1.

2.2. Geochemical analysis

The sediments were sieved through 1 mm sieve, oven dried at 45ºC and mechanically homogenized in an agate mill to avoid metal contamination. Metal concentrations were determined by Inductively Couple Plasma–Optic Emission Spectrometry (ICP-OES) after microwave digestion with aqua regia. Lowest detection limits were 0.1 mg kg^{-1} for Sc, 1 mg kg^{-1} for Mn, Zn, Cu and Ni, 2 mg kg^{-1} for Pb and Cr, 3 mg kg^{-1} for As and 0.01% for Fe and Ca.

As described above, sediments from the Muskiz estuary exhibit substantial granulometric variations. Therefore, it was essential to normalize them to exclude the effects of grain size in order to provide a basis for meaningful comparisons (ICES, 1989). Different elements (Fe, Mn, Al, Li…) have been proposed as suitable factors for geochemical normalization (OSPAR, 1998). In this work Sc was chosen as grain proxy because it exhibits a reasonably close relationship with Fe (Pearson´s correlation coefficient, r=0.77), Mn (r=0.75), Zn (r=0.83), Pb (r=0.72), Cu (r=0.81), Ni (r=0.93), Cr (r=0.82) and As (0.70) in samples from both analyzed cores (n=41).

2.3. PAH analysis

Approximately 1 gram of dry sediment was weighed and transferred to a Teflon lined extraction vessel together with 1 g of activated copper to eliminate the possible presence of sulphur in the sample. The sample was spiked with 25 µl of a mixture of acenaphthene-d_{10}, chrysene-d_{12} and phenanthrene-d_{10} at 20 µg ml^{-1} in acetone. Finally, 15 ml of acetone were added to the sample and the extraction was performed in a MDS-2000 microwave (CEM, Matthews, NC, USA) at 21 psi for 15 min at 80% of the maximum microwave power (Bartolomé *et al.*, 2005).

The supernatant liquid was filtered through PTFE filters (25 mm, 5 µm, Waters trade mark) and the extract was concentrated to about 0.5 ml using nitrogen blowdown evaporation after the addition of aproximately 1 ml of *iso*-octane. *Iso*-octane was added in order to minimise losses during the evaporation process and to assure that the concentrated extract was in a non-polar solvent before the solid phase extraction (SPE) clean-up step in Florisil® cartridges. The concentrated extract was loaded onto a 1 g Florisil® cartridge, which had been previously rinsed with 4 ml of *n*-hexane. The test tube was rinsed with another 0.5 ml of *n*-hexane which were also loaded onto the Florisil® cartridge. The cartridge was eluted with 12 ml of a (4:1) *n*-hexane:toluene mixture (PAHs and PCBs). The eluates were concentrated to dryness and re-dissolved in 500 µl of *iso*-octane.

The extracts were analyzed in a 6890N Agilent gas chromatograph coupled to a 5973N Agilent mass spectrometer (Agilent Technologies, Avondale, PA, USA) with a 7683 Agilent autosampler. Two µl of sample were injected in the splitless mode at 270ºC into a HP-5 capillary column (30 m x 0.25 mm x 0.25 µm, Agilent Technologies). The mass spectrometer was operated in the electron impact ionisation mode, the interface was kept at 300ºC and the ionisation source and the quadrupole at 230ºC and 150ºC, respectively. Measurements were performed in the SIM mode (Table 1). The method was validated using the NIST 1944 certified marine sediment.

Blank samples were processed in the same way as the sediment samples in order to estimate the detection limits. Some of the sediment samples were analyzed in duplicate to check the repeatability of the method. The detection limits and relative standard deviations estimated in this way for each analyte are included in Table 1. In all, 16 surface samples were studied from the estuarine tidal flats and 14 samples were analyzed from Core B.

2.4. ^{210}Pb and ^{137}Cs analysis

Core samples were dried, first at room temperature and then oven-dried at 110º C for twenty four hours. Once dry, samples were broken up and passed through a 2 mm sieve. They were then placed in closed plastic containers in order to obtain the radioactive equilibrium between ^{226}Ra and ^{222}Rn daughters over thirty days.

The determination of the concentration of existing radioactive isotopes in each sample was carried out by low-background gamma spectrometry with a vertically configured Ge HP detector. This detector was connected to a container holding liquid nitrogen by a cold finger and it was mounted inside a 10 cm lead shielding against room and cosmic background. The detector was also linked to an electronic chain, which in turn is connected to a multichannel analyser (Quindós *et al.*, 1994).

PAH	m/z	Detection limit	%RSD
Nap	128, 129	0.99	3.0-34.5
Acy	153	1.07	2.0-10.4
Ace	153, 154	2.01	5.0-12.8
Flu	165, 166	4.78	0.3-4.8
Phe	178, 179	1.29	2.4-8.6
Ant	178, 179	1.66	0.5-13.3
Fl	202, 203	9.72	1.4-11.3
Pyr	202, 203	11.20	1.1-8.1
B[a]A	228, 229	22.05	1.2-8.6
Chr	228, 229	0.56	0.1-8.4
B[b]F	252, 253	11.00	2.0-15.4
B[k]F	252, 253	9.19	1.3-14.1
B[a]P	252, 253	11.19	1.0-13.5
InP	276, 277	10.38	0.5-10.2
D[ah]A	276, 277	6.12	1.3-16.3
B[ghi]P	276, 277	4.42	0.8-16.9

Table 1.- Molecular ions used to quantify the micro-organic compounds (m/z) by GC/MS; detection limits (mg kg^{-1}) and relative standard deviations (%RSD) estimated for each organic analyte. Detection limits were estimated as three times the signal of the blank.

Table 1.- Iones moleculares utilizados en la cuantificación de los compuestos micro-orgánicos (m/z) mediante GC/MS, límites de detección (mg kg^{-1}) y desviaciones estándar relativas (%RSD) estimadas para cada analito orgánico. Los límites de detección fueron estimados como tres veces la señal del blanco analítico.

The concentrations of the radioactive elements ^{137}Cs, ^{226}Ra and ^{210}Pb were determined by the number of counts beneath the corresponding photopeaks, taken into account background noise and spectrum base line. The photopeaks considered here are: 661 KeV from the ^{137}Cs, 46.5 KeV from the ^{210}Pb, 352 and 611 KeV from the ^{214}Pb and ^{214}Bi, daughter products of the ^{222}Rn in equilibrium with the ^{226}Ra (Lederer *et al.*, 1967). Each sample was counted for a period of twenty four hours. The detection efficiency of the measuring system was calculated using samples of known activity prepared with the same geometry as the samples to be measured. The uncertainties of the measured concentrations are due mainly to the statistical counting error, and depend on each value. In the used conditions for mass, geometry and twenty-four -hours time interval, the lower detection limits were 10 Bq Kg^{-1}, 3 Bq Kg^{-1} and 0.5 Bq Kg^{-1} for ^{210}Pb, ^{226}Ra and ^{137}Cs respectively.

3. The modern environment

3.1. Microfaunal content

The standing crop is the number of living individuals present per unit volume of a sediment surface (Murray, 1991). On the intertidal flats of the Muskiz estuary, standing crops (10 cm^3) show an increase from the upper to the middle i.e. estuary towards the sea, and then decrease abruptly in the sandy lower estuarine sediments (Fig. 2, Table 2). Foraminiferal abundance is very low and ranges from 1 (sample 1) to 70 (sample 13) with an average value of 25 individuals (Fig. 2). Samples 10 and 11, from the muddy middle estuary, exhibit a significative decrease in the foraminiferal absolute abundances. Both uppermost (samples 1-4) and lowermost (samples 16-17) localities in the estuarine intertidal flats contained less than 100 living individuals and consequently the results have not been considered quantitatively.

During the sampling period 30 different species of benthic foraminifera were found living on the intertidal flat (Appendix 1), although the maximum number of species at any one sampling station was only 19 (Fig. 2). In general, number of species increased accordingly to the standing crop from the upper estuary to the sea. The most abundant species found were *Ammonia tepida* and *Haynesina germanica* (Table 2). Living assemblages were dominated by calcareous hyaline foraminifera (always more than 55%) although in all samples from the the upper and middle estuary there was a variable amount of agglutinated forms, represented by the species *Jadammina macrescens* and *Trochammina inflata* (Table 2). The lower half of the estuary contains also a significative amount of porcellaneous forms, with important amounts of the species *Quinqueloculina seminula* (Table 2).

Fifty five different species of benthic foraminifera were found in the dead assemblages (Appendix 1). Uppermost (samples 1-3) localities contained less than 100 foraminiferal tests and consequently the results have not been considered quantitatively. Dead assemblages in the estuarine intertidal flats were also dominated by the same species that were dominant as living: *A. tepida*, *H. germanica*, *J. macrescens*, *T. inflata* and *Q. seminula* (Table 2). The inner shelf hyaline species *Rosalina irregularis* and *Cibicides lobatulus* are also highly abundant, being particularly concentrated in the lower half of the estuary. Other transported allochthonous species, found mainly as dead tests (such as porcellaneous *Quinqueloculina lata* and *Massilina secans*), tend to be more common in the lower reaches of the estuary. The number of dead species (average 8, 21, and 22 species in the upper, middle and lower estuary respectively), allochthonous foraminif-

era abundance (average 3%, 37%, and 80% in the upper, middle and lower estuary respectively), and the sand content increases steadily towards the estuary mouth suggesting the inner shelf as the main source of the abundant foraminiferal tests transported into the estuary, particularly in the sandy lower estuarine area. In general, hyaline foraminifera are dominant throughout the intertidal flats (average 67%), agglutinated tests are abundant in the upper and middle estuary (average 26%), and porcellaneous species are located more abundantly in the lower estuary (average 33%).

The living and dead species assemblages were similar in terms of dominant species, although the latter contains a higher number of tests and species as a consequence of the cumulative effects of annual production and transport of foraminifera from the open sea (Fig. 2, Table 2). Comparison of both assemblages for the same sample on a species by species basis, using the similarity index de-

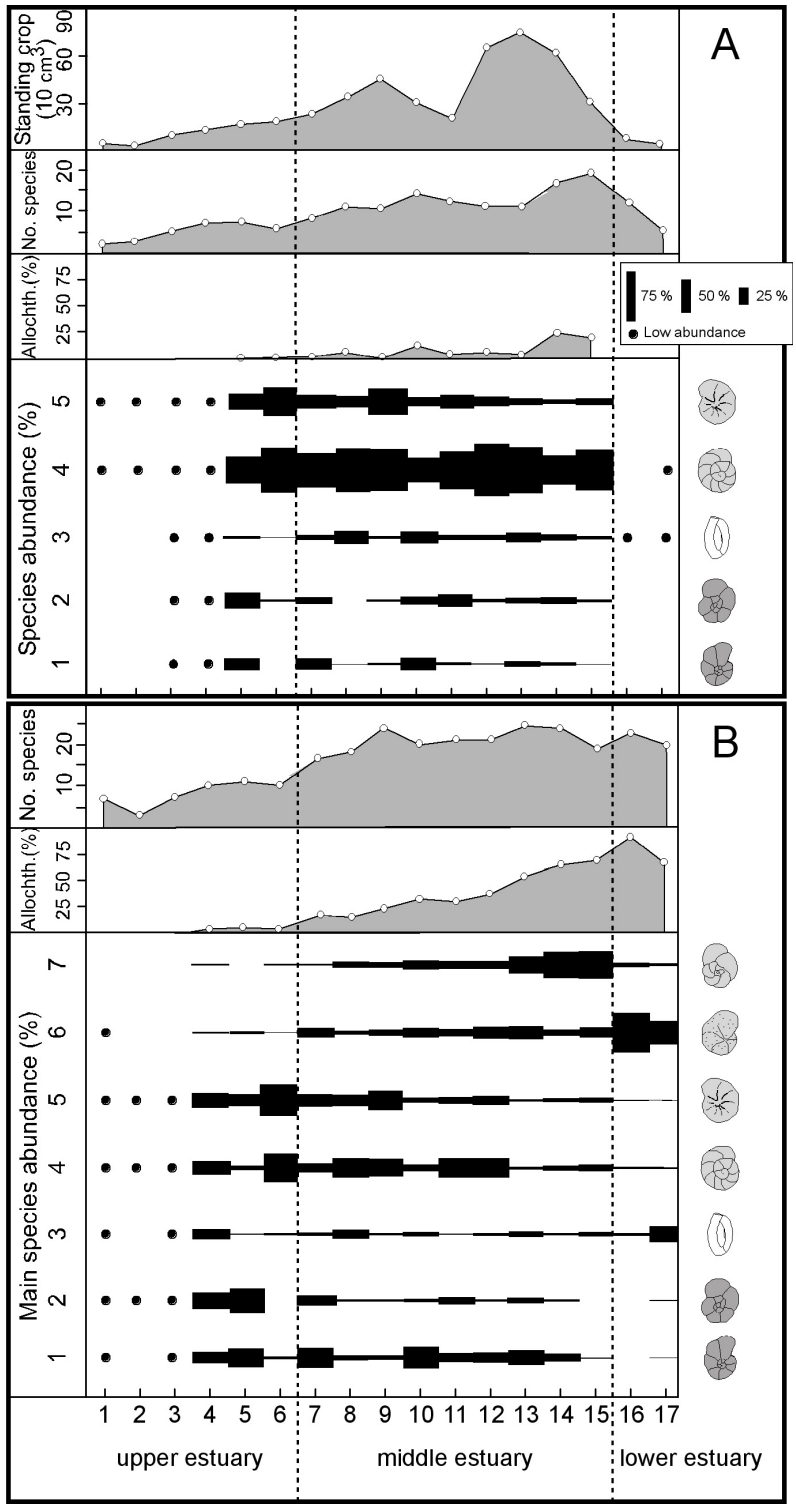

Fig. 2.- Abundance and composition of living (A) and dead (B) foraminiferal assemblages in surface sediment samples from the Muskiz estuary intertidal flats. 1: *J. macrescens*; 2: *T. inflata*; 3: *Q. seminula*; 4: *A. tepida*; 5: *H. germanica*; 6: *C. lobatulus*; 7: *R. irregularis*.

Fig. 2.- Abundancia y composición de las asociaciones vivas (A) y muertas (B) de foraminíferos en las muestras superficiales del canal estuarino de Muskiz. 1: *J. macrescens*; 2: *T. inflata*; 3: *Q. seminula*; 4: *A. tepida*; 5: *H. germanica*; 6: *C. lobatulus*; 7: *R. irregularis*.

Upper estuary	Middle estuary	Lower estuary
length: 3 km lithology: gravels (4%), sands (50%) and muds (46%) samples: 1-6	length: 2,3 km lithology: muds (60%) and sands (40%) samples: 7-15	length: 0,3 km lithology: sands (100%) samples: 16-17
9 (1-16) individuals 10 cm^{-3} 5 (2-7) L species L *A. tepida* 45 (33-58) % L *H. germanica* 30 (21-38) %	41 (18-70) individuals 10 cm^{-3} 13 (9-19) L species L *A. tepida* 50 (30-68) % L *H. germanica* 15 (7-36) % L *Q. seminula* 10 (4-19) % L *J. macrescens* 6 (0,4-17) % L *T. inflata* 5 (0-13) %	2 (1-3) individuals 10 cm^{-3} 9 (5-12) L species
8 (3-11) D species 3 (2-4) % allochthonous D *H. germanica* 28 (17-46) % D *A. tepida* 21 (5-41) % D *T. inflata* 21 (0-39) % D *J. macrescens* 16 (3-29) % L/D similarity: 73 (65-82) %	21 (17-24) D species 37 (13-70) % allochthonous D *A. tepida* 17 (4-29) % D *R. irregularis* 16 (1-39) % D *J. macrescens* 16 (1-33) % D *H. germanica* 13 (3-30) % D *C. lobatulus* 12 (5-19) % D *T. inflata* 5 (1-15) % D *Q. seminula* 5 (1-12) % L/D similarity: 52 (29-65) %	22 (20-23) D species 80 (68-91) % allochthonous D *C. lobatulus* 45 (33-57) % D *Q. seminula* 12 (3-22) % D *Q. lata* 11 (9-13) % D *M. secans* 6 (4-8) % L/D similarity: very low

Vegetated marsh	Tidal creek
lithology: mud samples: A2-3, B2-3, C2-4, D2-3, E4-6, F2-5, G2	lithology: sandy mud samples: A1, B1, C1, D1, E1-3, E7, F1, G1
154 (14-346) individuals 10 cm^{-3} 7 (2-11) L species L *T. inflata* 39 (10-72) % L *J. macrescens* 36 (12-60) % L *A. tepida* 12 (0-57) % L *C. williamsoni* 5 (0-20) % L *Q. seminula* 4 (0-15) %	83 (23-122) individuals 10 cm^{-3} 11 (6-15) L species L *A. tepida* 53 (31-73) % L *H. germanica* 16 (4-42) % L *J. macrescens* 10 (0,3-31) % L *C. williamsoni* 5 (3-11) % L *T. inflata* 4 (0,7-8) % L *Q. seminula* 3 (0-6) %
11 (2-29) D species 8 (0-54) % allochthonous D *J. macrescens* 55 (30-86) % D *T. inflata* 24 (0,3-59) % D *A. tepida* 8 (0-32) % D *C. lobatulus* 3 (0-18) % D *Q. seminula* 2 (0-15) % D *R. irregularis* 2 (0-13) % L/D similarity: 65 (30-90) %	23 (4-30) D species 55 (1-89) % allochthonous D *C. lobatulus* 26 (0.6-56) % D *J. macrescens* 12 (0,7-61) % D *R. irregularis* 12 (0-41) % D *H. germanica* 11 (1-55) % D *A. tepida* 11 (1-33) % D *Q. seminula* 5 (1-14) % L/D similarity: 42 (17-77) %

Table 2.- Summary of modern environment and microfaunal data. The single value represents the average and those in parentheses give the range. L: living, D: dead.

Table 2.- Síntesis de la información ambiental y microfaunística para las condiciones actuales. El valor individual representa la media y los valores entre paréntesis indican el rango. L: vivo, D: muerto.

fined by Rogers (1976), indicates a very high similarity for the upper estuary (average 73%), a moderate similarity in the middle estuary (average 52%) and a deduced very low similarity in the lower estuary (extremely low numbers of living foraminifera versus abundant allochthonous foraminiferal tests) (Table 2).

Duplicate sampling in September 2001 at some middle estuary locations (samples 8-12) showed results similar

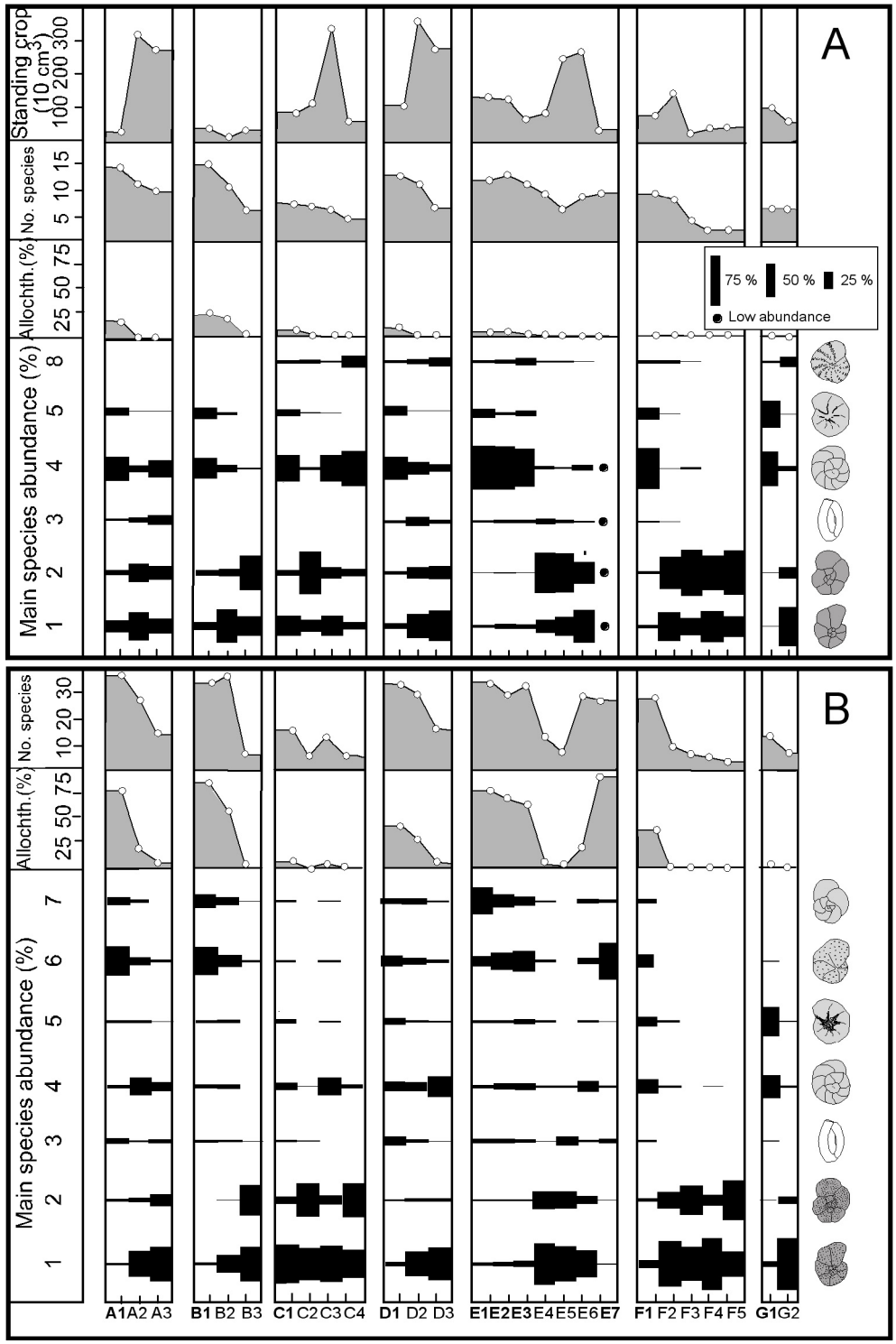

Fig. 3.- Abundance and composition of living (A) and dead (B) foraminiferal assemblages in surface sediment samples from the Muskiz estuary marsh. Tidal creek samples are in bold. 1: *J. macrescens*; 2: *T. inflata*; 3: *Q. seminula*; 4: *A. tepida*; 5: *H. germanica*; 6: *C. lobatulus*; 7: *R. irregularis*; 8: *C. williamsoni*.

Fig. 3.- Abundancia y composición de las asociaciones vivas (A) y muertas (B) de foraminíferos en las muestras superficiales de la marisma de Muskiz. Las muestras correspondientes a los canales de desagüe aparecen en negrita. 1: *J. macrescens*; 2: *T. inflata*; 3: *Q. seminula*; 4: *A. tepida*; 5: *H. germanica*; 6: *C. lobatulus*; 7: *R. irregularis*; 8: *C. williamsoni*.

to those of the previous sampling campaign (October-December 2000) in terms of species number and dominance. Standing crop (10 cm^3) values were higher in 2001 (average 109 individuals; range 60-162 individuals) than in 2000 (average 37 individuals; range 18-64 individuals) although minimum abundance values were detected again in samples 10 and 11 (Alday, 2004). These data are not included in the figures and tables.

Both absolute abundance and number of species ranges are similar in the vegetated and intertidal creek areas of the marsh (Table 2). The average standing crop (10 cm^3) values are 139 and 116 individuals respectively, showing a much higher foraminiferal abundance in the marsh than in the estuarine intertidal flats (Fig. 3). Only sample E7 contain less than 100 living individuals and its results could not be considered quantitatively.

	Surface samples (n=16)		Core B (n=24)		Core M (n=17)		Effect-range		CEDEX	
	M±D.S.	Range	M±D.S.	Range	M±D.S.	Range	ERL	ERM	I	III
(%)										
Ca	6.0±7.2	(1.5-30.5)								
Fe	7.5±3.0	(2.5-15.2)	5.3±1.1	(3.0-8.3)	4.8±2.3	(1.6-7.4)				
(mg kg^{-1})										
Mn	1490±395	(808-2274)	762±195	(525-1180)	1665±1030	(265-3029)	-	-		
Zn	171±60	(22-279)	187±59	(67-250)	165±99	(43-313)	150	410	500	3000
Pb	42±11	(11-56)	39±6	(24-48)	54±12	(35-74)	47	218	120	600
Cu	71±24	(21-118)	48±12	(17-62)	86±64	(7-190)	34	270	100	400
Cr	14±5	(4-24)	13±5	(5-23)	10±5	(4-19)	80	370	200	1000
Ni	31±9	(6-45)	26±4	(16-31)	29±15	(9-47)	21	52	100	400
As	19±9	(6-40)	14±5	(5-21)	41±15	(11-56)	8.2	70	80	200

ERL (Long *et al.*, 1995): concentrations below which adverse biological effects are rarely expected.
ERM (Long *et al.*, 1995): concentrations above which adverse biological effects are often observed.
CEDEX I (RGMD, 1994): concentrations below which sediments can be freely discharged into marine waters.
CEDEX III (RGMD, 1994): concentrations above which sediments must be treated to reduce pollution or isolated from the aquatic environment.

Table 3.- Average and concentration ranges of metals, As and Ca in sediments from the Muskiz estuary. Reference values proposed by Long *et al.,* (1995) and CEDEX (1994) have been also included. M±D.S. = Average plus standard variation.
Table 3.- Valor medio y rango de concentraciones de metales, As y Ca en los sedimentos del estuario de Muskiz. Se incluyen los valores de referencia propuestos por Long *et al.*, (1995) y CEDEX (1994). M±D.S. = Media más desviación estándar.

In all, 18 different species of benthic foraminifera were found living in the marsh (Appendix 1), although the average number of species was 7 and 11 in the vegetated and intertidal creek areas respectively. The most abundant species found were *A. tepida*, *H. germanica*, *J. macrescens*, *Cribroelphidium williamsoni* and *T. inflata* in the tidal creeks (Table 2). Living assemblages were dominated by a mixture of calcareous hyaline and agglutinated foraminifera similar to that found in the adjacent middle estuarine intertidal flats. However, more internal, elevated, and vegetated areas of the marsh are almost completely dominated by the agglutinated forms *T. inflata* and *J. macrescens* (Table 2).

Dead assemblages are much more abundant and diverse than their living counterparts. Fifty eight different species of benthic foraminifera were found in the dead assemblages (Appendix 1). In the tidal creek areas dead assemblages exhibit a very high allochthonous component (average 55 %), a very high number of species (average 23 species), and were dominated by *C. lobatulus*, *J. macrescens*, *R. irregularis*, *H. germanica*, *A. tepida* and *Q. seminula* (Table 2). Nevertheless, in the vegetated areas allochthonous transported foraminifera are scarce (average 8%), number of species is consequently moderate (average 11 species), and the dead assemblages are markedly dominated by *J. macrescens* and *T. inflata*.

Comparison of both assemblages for the same samples shows that in the intertidal creek areas foraminiferal contents are more variable (average similarity 42 %) due to the greater influence of the tides and currents that enter the marsh from the sea transporting allochthonous tests (Fig. 1) whereas the more elevated and vegetated areas exhibit a higher similarity (average 65 %) as these are less influenced by tidal inundation (Table 2).

3.2. Geochemical analysis

Summary statistics for the geochemical composition of surface samples are given in Table 3. The ranges of concentrations obtained for most elements are in good agreement with those previously reported by local authorities (Gobierno Vasco, 1999). However, the maximum contents determined for As exhibit a two-fold enrichment when compared with these local references. When spatial patterns for elemental contents after normalization to Sc is represented (Fig. 4), no definite distribution trends can be observed.

3.3. PAH analysis

The total concentration of PAH (ΣPAH) ranges from 0.1 to 2.6 mg kg^{-1}. In order to calculate the total concentra-

	Ant/(Ant/phen)	BaA/(BaA+Chr)	Fl/(Fl+Py)	InP/(InP+BghiP)
average	0.28	0.53	0.53	0.56
st.dev.	0.14	0.09	0.12	0.03
max.	0.78	0.87	0.91	0.66
min.	0.10	0.41	0.28	0.51

Table 4.- Average, maximum and minimum PAH isomer pair ratio values from the Muskiz estuarine tidal flat.
Table 4.- Valores de la relación media, máxima y mínima entre pares de isómeros PAH en el canal estuarino de Muskiz.

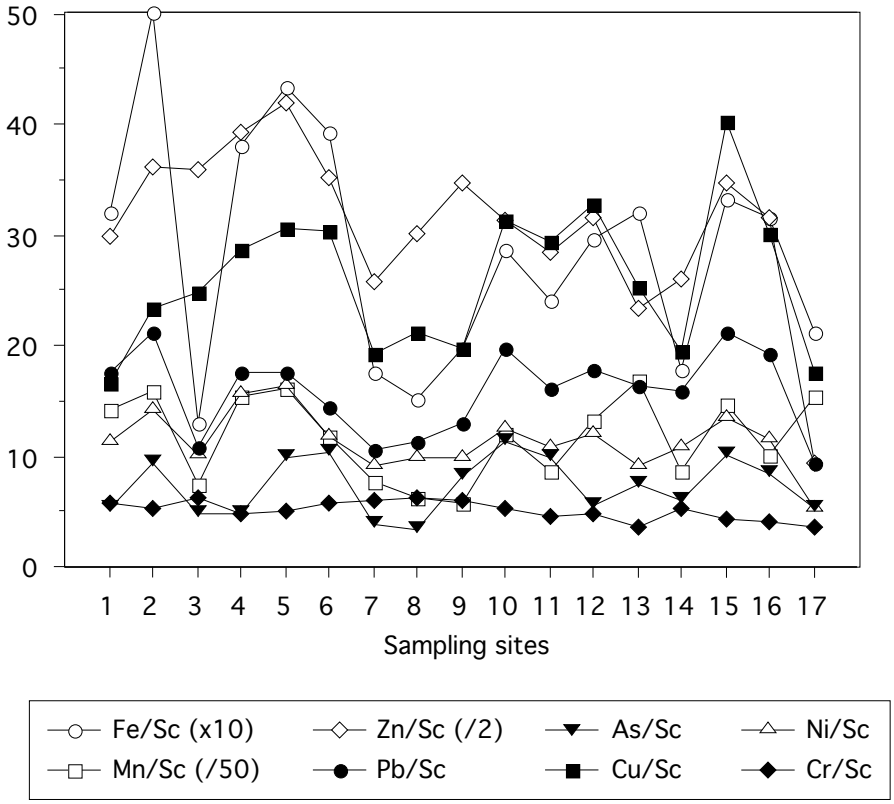

Fig. 4.- Sc-normalized concentrations of metals and As in surface sediments from the Muskiz estuary. Normalized values for Fe, Mn and Zn have been adapted (x10, /50 and /2 respectively) for representation purposes.
Fig. 4.- Concentraciones Sc-normalizadas de metales y As en sedimentos superficiales de la Ría de Muskiz. Los valores normalizados para el Fe, Mn y Zn han sido adaptados (x10, /50 y /2 respectivamente) para facilitar su representación gráfica.

tion of each group of contaminants, the concentration of each congener or isomer was taken into account, including the values below the detection limits. In these cases, instead of assigning zeros, half of the detection limit was used as general criteria. The distribution of the total concentration of PAHs along the different sampling stations and the range of concentrations of each isomer are plotted in figure 5a-b.

The total concentrations of PAHs found in the Muskiz estuarine intertidal flats are very low, as can be seen in Fig. 5a. As a matter of fact, they are much lower than those values found in the nearby highly polluted Bilbao estuary (0.5-328 mg kg^{-1}, Bartolomé *et al.*, 2006) and, surprisingly, even lower than concentrations obtained from the slightly polluted Urdaibai estuary (0.7-2.7 mg kg^{-1}, Bartolomé *et al.*, 2006).

If the distribution pattern of the individual isomers is taken into account, all the stations of the Muskiz intertidal flats showed a similar pattern, as can be seen in Fig 5b. As regards to the individual isomers, the heavier Fl, Pyr, BaA, Chr and BbF are the most predominant species while the lighter ones, i.e. Nap, Acy, Ace and Flu, occurred to be mostly below the detection limits as has also been observed in other nearby estuaries. Only sample 11 seemed not to fit into the general pattern since much lower concentrations were found (ΣPAH < 0.1 mg kg^{-1}). Moreover, if the distribution of each isomer is followed, the heaviest PAHs are predominant in this sample (InP, BahA and BghiP).

In order to get a better insight on the distribution of the isomers, a principal component analysis (PCA) was carried out by means of the Unscrambler program (Camo AS, Trondheim, Norway). From this analysis, excluding sample 11, the first three components explained up to 84% of the total variance. Since the first PC (66% of the total variance) was clearly linked to the total concen-

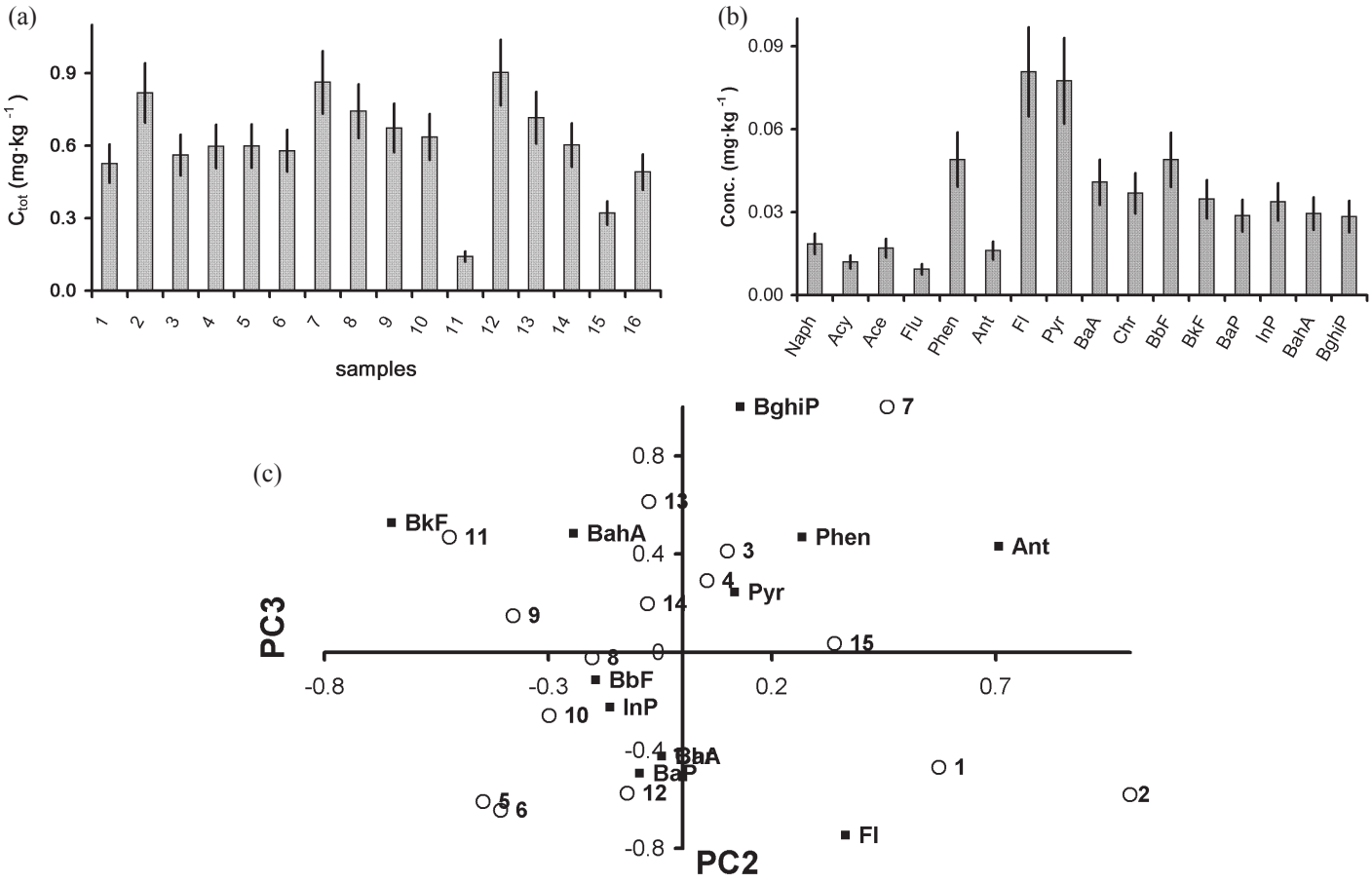

Fig. 5.- (a) Total concentration (mg kg^{-1}) of PAHs along the different sampling sites in the Muskiz estuarine intertidal flats; (b) distribution of the different PAHs measured in sampling site 3; and (c) biplot of PC2 against PC3, where the distribution of the samples and the PAHs are overlaid. The error bar stands for the expected overall uncertainty of the analysis (relative standard deviation of 15%).

Fig. 5.- (a) Concentración total de PAHs (mg kg^{-1}) en las diferentes muestras a lo largo del canal estuarino de Muskiz; (b) distribución de los diferentes PAHs medidos en la muestra 3; y (c) biplot de PC2 frente a PC3, donde se superponen las distribuciones de las muestras y de los PAHs. Las barras de error indicar la incertidumbre esperada en los análisis (desviación estándar relativa del 15%).

tration of PAHs, the second and third components (16% and 9% of the total variance, respectively) can provide a more significative information about the distribution of the samples and the different PAHs, as shown in Fig. 5c. In that picture, the loadings and the scores of the second and third PCs have been overlaid and it can be seen how the samples enriched with lighter PAHs are grouped at the right side of the plot while those samples with heavier PAHs are placed at the left of the plot.

Based on the following PAH isomer pair ratios: Ant/(Ant+Phen), Be[a]A/(Be[a]A+Chr), Fl/(Fl+Py) and InP/(InP+BghiP), it is possible to suggest the sources of PAH in these sediments. Those four ratios have been determined from the estuarine intertidal flats sediment samples and were compared to the ratios corresponding to several major sources, i.e. environmental samples, petroleum and combustion, which were compiled by Yunker *et al.*, (2002). According to the ratio values obtained, Ant/(Ant+Phen) <0.10, Be[a]A/(Be[a]A+Chr) <0.20, Fl/(Fl+Py) <0.40 or InP/(InP+BghiP) <0.20 suggests dominance of petroleum; Be[a]A/(Be[a]A+Chr) 0.20-0.35, Fl/(Fl+Py) 0.40-0.50 or InP/(InP+BghiP) 0.20-0.50 indicates combustion or petroleum; and finally, Ant/(Ant+Phen) >0.10, Be[a]A/(Be[a]A+Chr) >0.35, Fl/(Fl+Py) >0.50 or InP/(InP+BghiP) >0.50 suggests combustion of coal, grass and wood. The average ratio values and the maximum and minimum values from this estuary are summarized in Table 4. The high ratios, together with the narrow range of the values, are consistent with a common source for all the samples in the estuarine intertidal flats: the combustion of petroleum, coal or wood. As it was stated above, station 11 has an outstanding value in two of the four indexes, which suggests a specific episode of high contamination.

3.4. Environmental interpretation

Petroleum refinery wastewaters are composed of many different chemicals which include oil and greases, phe-

nols, sulphides, ammonia, suspended oils, cyanides, nitrogen compounds and heavy metals. Nevertheless, the chemicals that have been identified as being the most likely cause of the toxicity are the PAHs. Refinery effluents tend to have fewer of the lighter hydrocarbons than crude oil but more polycyclic aromatics which tend to be more toxic and more persistent in the environment. Each refinery effluent is generally unique (components of the original crude oil, the resultants from the fractionation process, plus chemical additives within the refinery operations) and can vary on a daily basis depending on which units within the refinery are in operation. Also, it must be considered that the low salinity of the effluent might be an important factor for causing the impact to the area rather than the oil. The exact effects of refinery effluents and its constituents can and do vary between species and from location to location (Wake, 2005).

The results obtained from the surface samples indicate that, in the Muskiz estuary, concentrations of metals and As are low and similar to those determined in sediments from the nearby and moderately polluted Plentzia estuary (Seebold, 1981; Irabien, 1993). In the same way, PAHs concentrations in these sediments are very low and even lower than concentrations obtained from the nearby slightly polluted Urdaibai estuary (Bartolomé *et al.*, 2006). Only station 11 (middle estuary) has an outstanding value in two of the four indexes, which suggests a specific episode of high contamination. Therefore, the Muskiz estuary shows a moderate level of pollution confirming previous studies of surface sediments (Gobierno Vasco, 1998b and 1999).

However, although the marsh sediments exhibit similar foraminiferal contents to those of other nearby marshes on the adjacent coast, the biological response shows, in general, very low foraminiferal abundance and species number along the estuarine intertidal flats with increasing values towards the sea from the upper to the middle estuary, and which then decrease abruptly in the sandy lower estuarine area. Only samples 10 and 11, located in the muddy middle estuary, exhibit a significative reduction in their living foraminiferal absolute abundances and perhaps this is related to effluent discharge in these particular areas. García-Arberas (1999) studied the intertidal zoobenthic communities in this estuary tidal flats and concluded that they were much less abundant and diverse than those from the well preserved Plentzia and Urdaibai estuaries and this was due to the unusually low nutrient contents in the sediments.

Consequently, it can be concluded that low abundance and species number values observed in the microfauna do not seem to be due to the persistent pollution in the estuary. More likely, these seem to be the consequence of the systematic destruction of the original estuarine environments to establish the oil refinery; this resulted in the reduction of the estuary to practically a mere estuarine channel and, therefore, the impoverishment of its general environmental quality.

4. Historical evolution

Whereas surface sediment samples provided information on the current microfaunal and geochemical characteristics of the modern estuarine environments, information on the historical change which has occurred in response to land reclamation and oil refinery activities in the area was obtained by studying variations in foraminiferal assemblages and geochemical composition of two short sediment cores.

Core B was obtained from a small intertidal mudflat in the middle estuary (Fig. 1). The sediment was black and stinking, with the upper oxidized 1 cm brown in colour. It was composed of muddy sediment with increasing sand contents downcore. Photography and X-ray radiograph revealed that the sediments are finely-laminated, with burrows of polychaetes (*Hediste diversicolor*) in the uppermost 10 cm (Fig. 6). Core M was recovered in the central part of the Muskiz marsh (Fig. 1). Most of the sediment is sandy and bioclastic except for the upper 16 cm that are composed of burrowed muddy, laminated sediment richer in vegetal organic matter (Fig. 7).

4.1. Microfaunal content

The number of benthic foraminifera present in the Muskiz intertidal flats core (B) is high and shows a general upward decrease in abundance following the distribution of the sand content. In total, more than 9,000 foraminiferal tests were obtained in the 51 samples analyzed. Foraminiferal results in Fig. 6 are expressed as number of foraminiferal tests per g of dry sediment for standardisation. Fifty nine different species were found in this core (Appendix 1).

Four distinct foraminiferal assemblage zones (FAZ) can be distinguished at different depths in the composite core. The basal 62 cm (100-36 cm depth interval) is made of dark-brown sandy sediment with abundant bioclasts, and it is characterized by an extremely high dominance of allochthonous foraminifera transported from the inner shelf (average 92%). This foraminiferal assemblage is dominated by very abundant *C. lobatulus*, and secondary *Q. lata*, *Rosalina anomala*, *R. irregularis* and *A. tepida*. This FAZ1 contains the highest number of tests g^{-1} in the core (average 145) and species (average number of species 26). The sand content is high (average 59%). By compar-

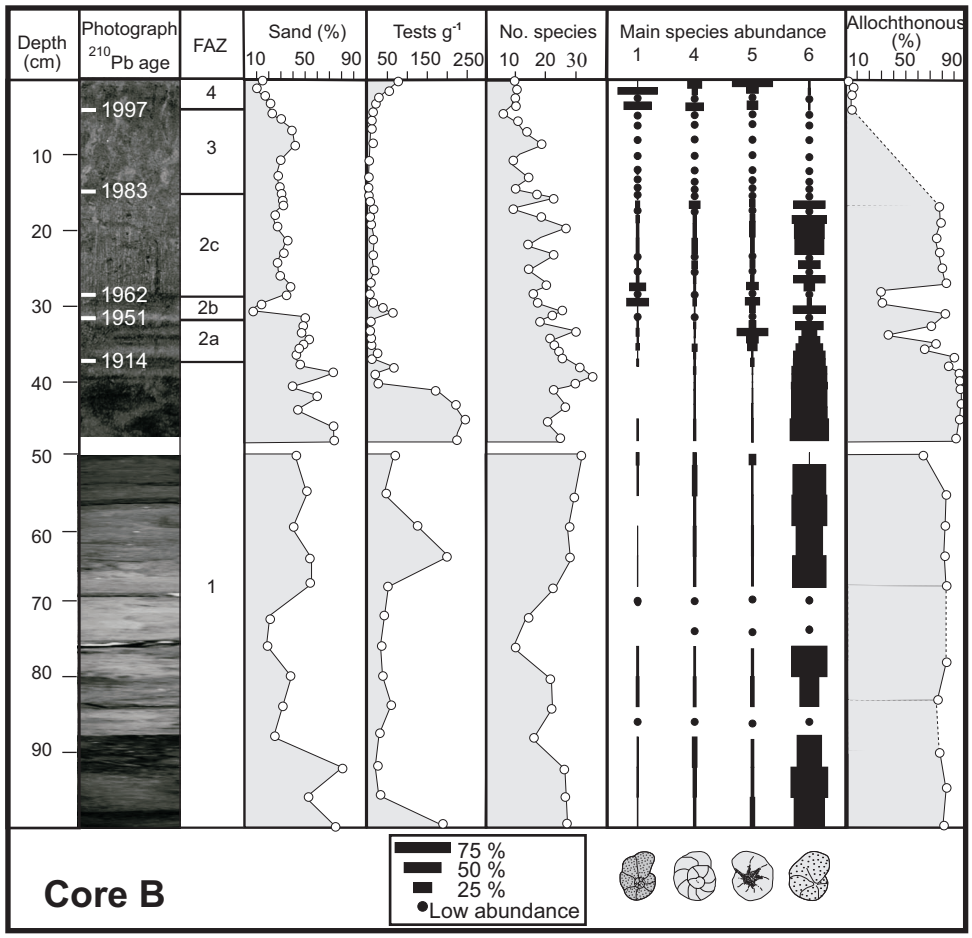

Fig. 6.- Photograph, ^{210}Pb age, sand content (%), foraminiferal abundance and number of species, main foraminiferal species (1: *J. macrescens*; 4: *A. tepida*; 5: *H. germanica*; 6: *C. lobatulus*) and allochthonous foraminiferal content (%) with depth (cm) in the Muskiz estuary tidal flats composite core B.

Fig. 6.- Fotografía, contenido en arena (%), abundancia y número de especies de foraminíferos, principales especies de foraminíferos (1: *J. macrescens*; 4: *A. tepida*; 5: *H. germanica*; 6: *C. lobatulus*) y contenido en foraminíferos alóctonos (%) en función de la profundidad (cm) para el pequeño sondeo compuesto B del canal estuarino de Muskiz.

ison with modern assemblages in the Muskiz estuary and elsewhere, this FAZ1 has been interpreted as having been deposited on an intertidal sandy flat with normal marine salinity conditions (Fig. 6 and Table 5).

The succeeding 21 cm of dark muddy sediment are characterized by FAZ2. This zone has been divided into three distinct subzones based on its foraminiferal content. Subzone 2a, from 36 to 30 cm depth, exhibits an abrupt decrease in foraminiferal abundance (average 11 individuals g^{-1}) although the number of species is similar than in the previous zone (average number of species 24). Both the sand content (average 47%) and the allochthonous foraminiferal abundance (average 65%) are lower than in FAZ1. The most important species are *C. lobatulus* and *H. germanica* together with minor *R. irregularis*. Comparison with the modern assemblages indicates this FAZ2 as a sandy mud brackish environment well connected to the open sea.

The next 3 cm are characterized by FAZ2b. This subzone is dominated by typical estuarine species as *J. macrescens*, *H. germanica* and *A. tepida*, whereas allochthonous species as *C. lobatulus* and *R. irregularis* show lower abundances (Fig. 6 and Table 5). The sand content decreases significatively in this interval (average 17%) together with the allochthonous component (average 29%). Foraminiferal density g^{-1} is slightly higher (average 26) and number of species is lower (average 16 species) than in the previous subzone. By comparison with modern assemblages, this FAZ2b is interpreted as a low brackish marsh subenvironment.

Subzone 2c, from 27 to 15 cm depth, shows an increase in sand (average 29%) and a decrease in foraminiferal (average 10 tests g^{-1}) contents with values similar to FAZ2a. Number of species is moderate (average 18 species) and several samples contain less than 100 foraminiferal tests. Assemblages are dominated by allochthonous foraminif-

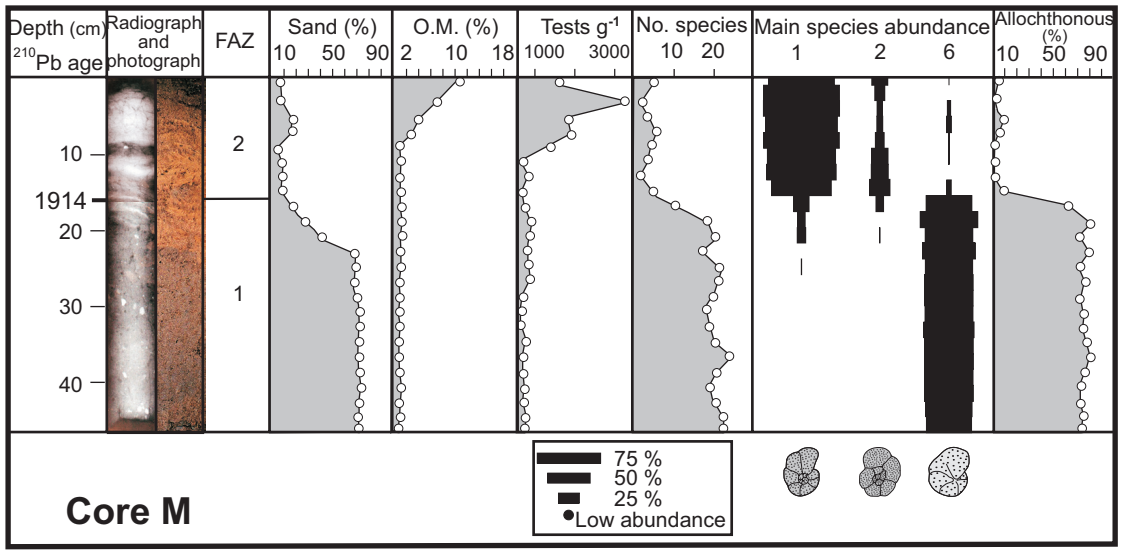

Fig. 7.- Photograph and X-radiograph, ^{210}Pb age, sand content (%), organic matter content (%), foraminiferal abundance and number of species, of main foraminiferal species (1: *J. macrescens*; 2: *T. inflata*; 6: *C. lobatulus*) and allochthonous foraminiferal content (%) with depth (cm) in the Muskiz marsh core M.

Fig. 7.- Fotografía y radiografía, contenido en arena (%), contenido en materia orgánica (%), abundancia y número de especies de foraminíferos, principales especies de foraminíferos (1: *J. macrescens*; 2: *T. inflata*; 6: *C. lobatulus*) y contenido en foraminíferos alóctonos (%) en función de la profundidad (cm) en el pequeño sondeo M de la marisma de Muskiz.

Core B

FAZ1	FAZ2a	FAZ2b	FAZ2c
depth interval: 100-36 cm thickness: >64 cm lithology: sand with bioclasts 59 (38-75) % sand	depth interval: 36-30 cm thickness: 6 cm lithology: sandy mud 47 (41-55) % sand	depth interval: 30-27 cm thickness: 3 cm lithology: mud 17 (6-35) % sand	depth interval: 27-15 cm thickness: 12 m lithology: sandy mud 29 (23-39) % sand
145 (14-240) tests g^{-1} 26 (20-35) species 92 (82-95)% allochthonous *C. lobatulus* 60 (54-67) % *Q. lata* 7 (4-10) % *R. anomala* 4 (2-5) % *R. irregularis* 3 (1-10) % *A. tepida* 3 (2-4) %	11 (4-26) tests g^{-1} 24 (17-30) species 65 (34-82) % allochthonous *C. lobatulus* 42 (25-56) % *H. germanica* 22 (10-52) % *R. irregularis* 7 (1-26) %	26 (8-57) tests g^{-1} 16 (15-17) species 29 (28-29) % allochthonous *J. macrescens* 30 (26-35) % *H. germanica* 22 (20-25) % *C. lobatulus* 13 (7-18) % *A. tepida* 12 (6-18) % *R. irregularis* 7 (4-11) %	10 (5-17) tests g^{-1} 18 (9-27) species 77 (73-82)% allochthonous *C. lobatulus* 51 (37-59) % *H. germanica* 8 (6-9) % *A. tepida* 6 (3-9) % *R. anomala* 5 (3-9) %

Core B (cont.)

FAZ3	FAZ4
depth interval: 15-4 cm thickness: 11 cm lithology: sandy mud 32 (22-41) % sand	depth interval: 4-0 cm thickness: 4 cm lithology: mud 15 (9-21) % sand
5 (3-9) tests g^{-1} Few tests	39 (12-77) tests g^{-1} 9 (6-10) species 6 (4-7) % allochthonous *H. germanica* 35 (17-67) % *J. macrescens* 35 (1-63) % *A. tepida* 20 (8-29) %

Core M

FAZ1	FAZ2
depth interval: 47-16 cm thickness: >31 cm lithology: sand with bioclasts 66 (23-75) % sand 1.1 (0.6-1.6) % organic matter	depth interval: 16-0 cm thickness: 16 cm lithology: mud 11 (8-16) % sand 3.6 (0.9-10.9) % organic matter
277 (110-524) tests g^{-1} 25 (17-31) species 74 (62-81)% allochthonous *C. lobatulus* 57 (52-68) % *Q. lata* 6 (0,3-11) % *Q. seminula* 6 (0-8) %	1,299 (114-3,809) tests g^{-1} 5 (2-7) species 3 (0-7) % allochthonous *J. macrescens* 82 (70-89) % *T. inflata* 14 (7-23) %

Table 5.- Summary of core and microfaunal data. The single value represents the average and those in parentheses give the range

Table 5.- Síntesis de la información microfaunística en los pequeños sondeos. El valor individual representa la media y los valores entre paréntesis indican el rango.

era (average 77%) with very abundant *C. lobatulus*, and much lower contents of *H. germanica*, *A. tepida* and *R. anomala*. This FAZ2c represents a return to the sandy-mud brackish environment with good connections to the open sea that occured during deposition of Subzone 2a (Fig. 6 and Table 5).

The following 11 cm of the core contain extremely low amounts of foraminiferal tests (calculated average 5 tests g^{-1}) and a moderate sand content (average 32%). This interval FAZ3 did not contain enough tests for calculations and the represented species are *A. tepida*, *H. germanica*, *J. macrescens* and *C. lobatulus*.

Finally, the top 4 cm reflect the current environmental conditions in the middle estuary area, with low sand contents (average 15%), and a moderately abundant (average 39 individuals g^{-1}) and poorly diversified (average 9 species) foraminiferal assemblage (FAZ4). Allochthonous species are very scarce (average 6%) and both hyaline and agglutinated species are dominant: *H. germanica*, *J. macrescens* and *A. tepida* (Fig. 6 and Table 5).

On the other hand, the number of benthic foraminifera present in the Muskiz marsh core (M) is very high and this show a general upward increase in abundance following the reduction of the sand content (Fig. 7). In total, more than 7,000 foraminiferal tests were obtained in the 23 samples analyzed.

Forty six different species were found in this core (Appendix 1) and two distinct foraminiferal assemblage zones can be distinguished in Core M. The basal 31 cm (47-16 cm depth interval) are made of dark-brown sandy sediment with abundant bioclasts, and these are characterized by a high dominance of transported, allochthonous foraminifera (average 74%). The foraminiferal assemblage is dominated by abundant *C. lobatulus*, and secondary *Q. lata* and *Q. seminula* (Table 5). This FAZ1 contains a high number of tests g^{-1} (average 277) and number of species (average 25 species). The sand content is also high (average 66%) and decreases significantly in the upper 5 cm of this zone when agglutinated, marsh foraminifera enter the assemblage. By comparison with modern assemblages in the Muskiz estuary and elsewhere, this FAZ1 has been interpreted as having been deposited in an intertidal sandy environment with normal marine salinity conditions, similar to FAZ1 of Core B described previously, that becomes progressively shallower throughout the last 5 cm of this zone (Fig. 7 and Table 5).

Finally, the top sixteen cm represent current environmental conditions in the vegetated marsh area, with very low sand contents (average 11%), extremetely abundant foraminiferal tests (average 1,299 individuals g^{-1}) and a very poorly diversified (average 5 species) foraminiferal assemblage (FAZ2). The content of organic matter flat). In the upper half of this core (Fig. 8) Sc-normalized contents for all the analyzed elements are similar to those found in surface samples, whereas two marked coincident peaks in concentrations can be observed in down-core samples at about 31 and 37 cm depth. The presence of metals from different anthropogenic sources, together with the presence of enhanced levels of redox-sensitive elements such as Fe and Mn, suggests that these enriched levels may be the result of post-depositional modifications due to early diagenetic effects. The redox cycles of Fe and Mn in sediments have been well documented over the last decades (Froelich *et al.*, 1979; Williams *et al.*, 1994; Thomson *et al.*, 1993, 2002). When oxygen become depleted in the sedimentary column, they may be dissolved, and released ions may migrate downwards (and be inmobilized due to sulfide formation) and upwards (and precipitate onto Fe- and Mn-oxyhydroxides in the oxic zone). Notwithstanding that the extent of early-diagenetic processes is difficult to assses without detailed geochemical studies of porewaters, some information can be inferred from the available data. If fixation of Fe and Mn (and other elements such as Zn, Pb, Cu, Cr, Ni and As, which all seem to behave in the same way in this core) occur in reducing conditions, an enrichment in S concentrations at the same depths would be expected. Nevertheless, vertical distribution patterns for this element exhibit a negative correlation with those displayed by the metals (Fig. 8), ruling out that the formation of sulfides causes them to bond in the sediment. Therefore, the observed peaks are more likely to be due to oxyhydroxide formation under oxidized conditions and migration of the diagenetic redox fronts.

On the other hand, vertical geochemical profiles for core M (illustrated in Fig. 9) show that below 10 cm depth, there is a sharp increase in Ca concentrations, which probably reflects the abundance of bioclasts. Although other European marshes exhibit a declining trend in Ca with depth due to decalcification (Cundy and Croudace, 1995; Spencer *et al.*, 2003; Zwolsman *et al.*, 1993), this distributional pattern is consistent with previous observations about the good preservation of calcareous species in recent sedimentary deposits of the northern coast of Spain (Cearreta and Murray, 2000; Cearreta *et al.*, 2002). Once the granulometric effect is adjusted for, a similar pattern with depth can be determined for Pb and this is probably related to this compositional change. On the contrary, normalized concentrations of Fe, Mn, Zn and Cu show an strong negative correlation with Ca (>0.80). Finally, Cr, Ni and As remain fairly constant throughout the whole core.

Both surface and core samples collected in Muskiz estuary exhibit moderate contents of metals which are lower

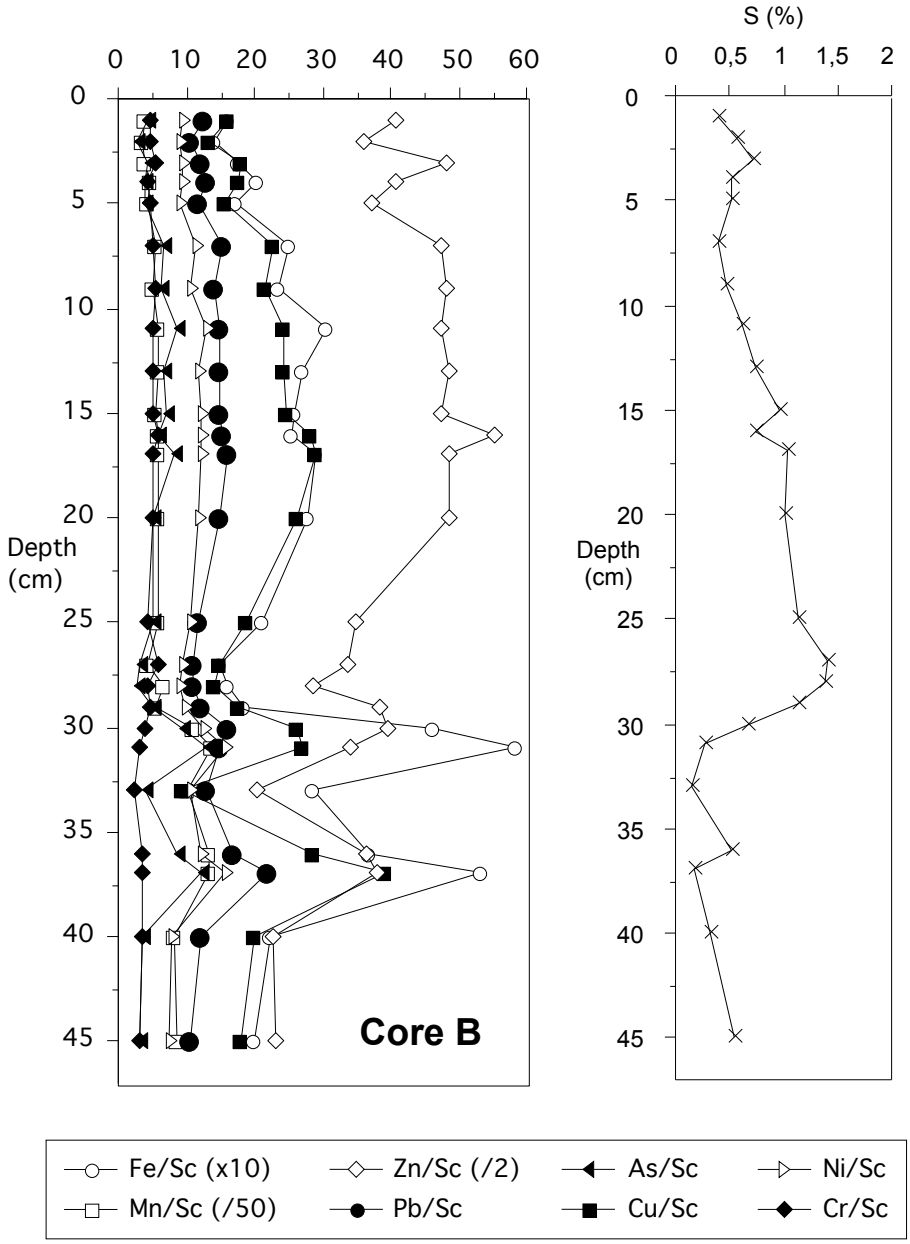

Fig. 8.- Sc-normalized concentrations of metals and As, and S contents (%) in sediments from core B. Normalized values for Fe, Mn and Zn have been adapted (x10, /50 and /2 respectively) for representation purposes.

Fig. 8.- Concentraciones Sc-normalizadas de metales y As, y contenido en S (%) en sedimentos del pequeño sondeo B. Los valores normalizados para el Fe, Mn y Zn han sido adaptados (x10, /50 y /2 respectivamente) para facilitar su representación gráfica.

that those of the highly polluted Bilbao estuary (Cearreta *et al.*, 2000) and similar or even lower than those found in the quite well preserved estuaries of Urdaibai (Irabien and Velasco, 1999) and Plentzia (Cearreta *et al.*, 2002). Due to the Spanish recommendations for the management of dredged materials (CEDEX, 1994, see Table 3), these sediments (except few samples from core M with high contents of Cu) should be placed under category I (non-contaminated and/or slightly contaminated). Applying the effects range approach proposed by Long *et al.,* (1995), which ranks all data for which a biological effect was observed in conjunction with an elevated contaminant content (Table 3), concentrations remain below the Effect-Range Median (ER-M). This value represent a threshold above which adverse effects on most species will frequently occur.

4.3. PAH analysis

From the Core B samples is not possible to determine a definitive trend in the pollution pattern (Fig. 10). Concentration of PAHs decreased in the first few cm reaching an almost constant value which suggests a continuous source of PAHs during the last few years.

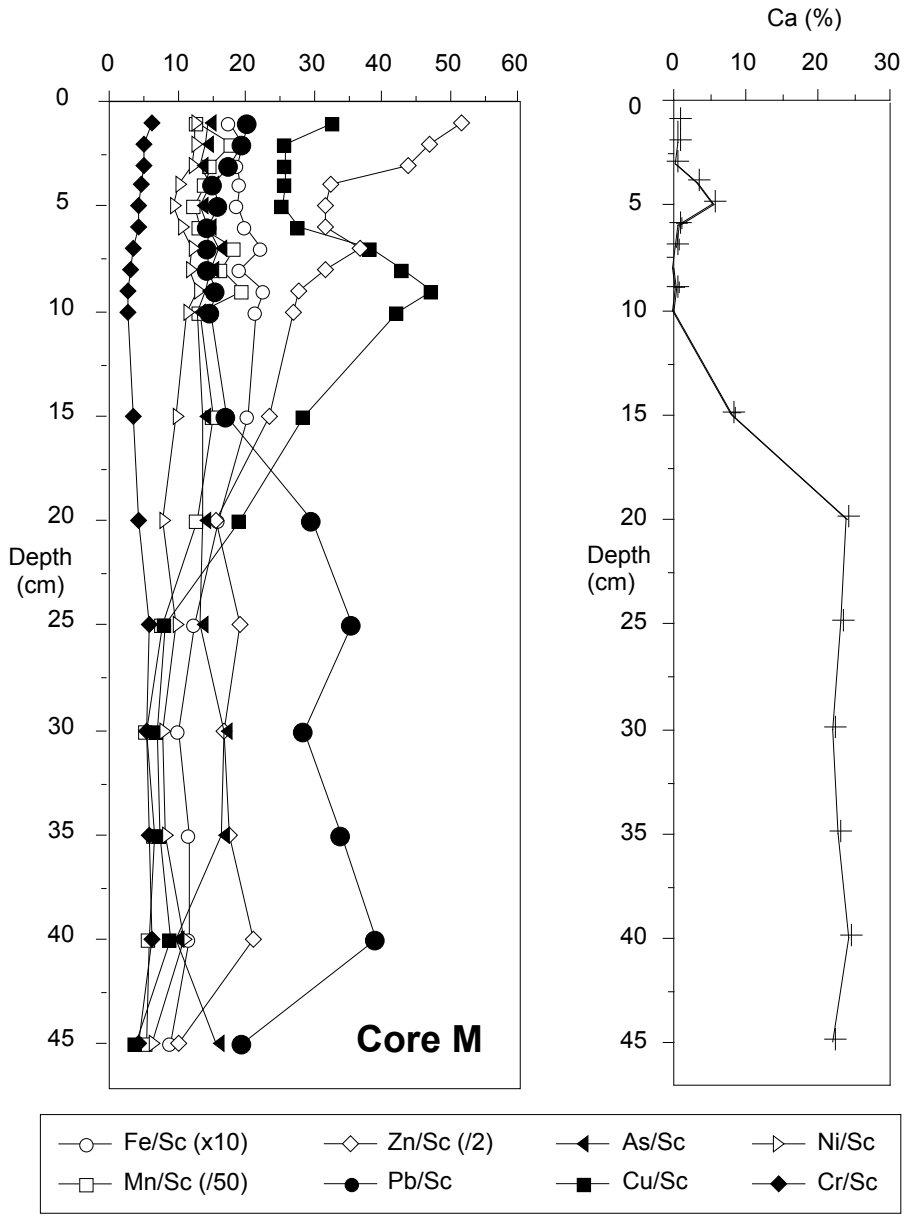

Fig. 9.- Sc-normalized concentrations of metals and As and Ca contents (%) in sediments from core M. Normalized values for Fe, Mn and Zn have been adapted (x10, /50 and /2 respectively) for representation purposes.

Fig. 9.- Concentraciones Sc-normalizadas de metales y As, y contenido en Ca (%) en sedimentos del pequeño sondeo M. Los valores normalizados para el Fe, Mn y Zn han sido adaptados (x10, /50 y /2 respectivamente) para facilitar su representación gráfica.

If the concentrations obtained for this core are compared to the guideline values given for the low-range and median range effects (Long *et al.*, 1995) it can be concluded that the concentrations in this sedimentary sequence are lower than the low-range effects (Table 6). Therefore, it is unlikely that the concentration of PAHs found in the Muskiz estuary have any effect on the biota.

4.4. ^{210}Pb and ^{137}Cs dating

In Core B, ^{137}Cs shows values around 5 Bq kg^{-1} that seem to be randomly distributed. After different statistical treatments two different maxima are present at -18 cm and -32 cm. Data were also fitted to a 3 grade polynomial curve and their distribution show a maximum around -28 cm depth (Fig. 11). Based on the ^{137}Cs behaviour, it can be deduced that the material corresponding to the first 28 cm has been deposited during approximately the last 39 years.

^{226}Ra exhibits a constant value around 16 Bq kg^{-1} that is considered as low. ^{210}Pb concentrations seem to decrease from 60 to 15 Bq kg^{-1} between -45 cm and the surface. Calculating the ^{210}Pb in excess, a decrease of its concentration in the surface has been found, although measurement uncertainties are high. Consequently, bearing in mind experimental errors, concentrations have been fitted

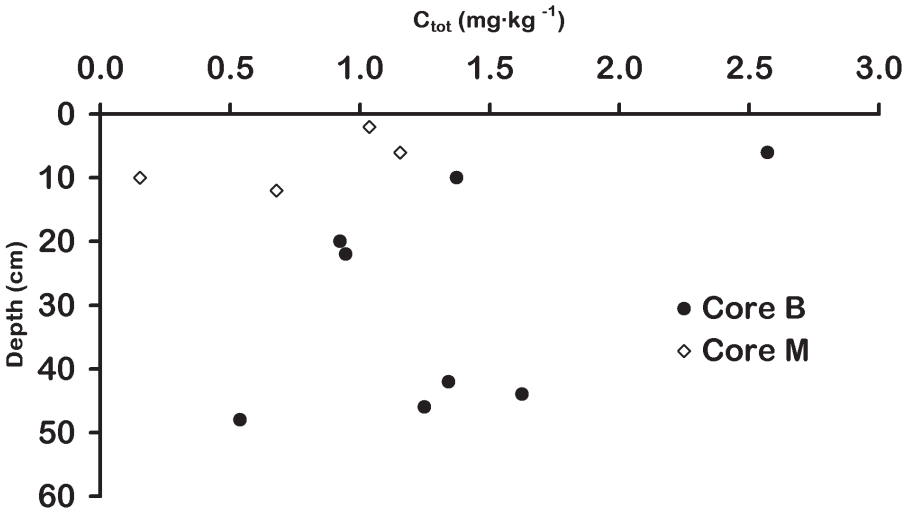

Fig. 10.- Concentration of PAHs (mg kg^{-1}) with depth (cm) in core B (tidal flat) and core M (marsh) from the Muskiz estuary.

Fig. 10.- Concentración de PAHs (mg kg^{-1}) en función de la profundidad (cm) en los pequeños sondeos B (canal principal) y M (marisma) de la Ría de Muskiz..

to a 3 grade polynomial function obtaining a low correlation coefficient. However, it has been considered that real values for ^{210}Pb in excess are correct (Fig. 11).

Using ^{210}Pb values in excess calculated for each depth of the fitted polynomial function, CIC (Constant Initial Concentration) and CRS (Constant Rate of Supply) models have been used to determine the age of the different samples. Ages obtained using the CIC model are very low compared to those obtained by the CRS model. In order to select which method should be more valid, ^{137}Cs values have been considered. Therefore, taking into account the age assigned to the -28 cm sample, it can be deduced that CRS model is most adequate and that ages obtained using this method are correct.

Based on the ages calculated by the CRS model, the historical evolution of the sedimentation rates has been estimated. This has been calculated relating sample thickness with ages determined for the top and bottom parts. As shown by Figure 11, sedimentation rates show an abrupt increase from 1930 to the present.

In Core M, ^{210}Pb in excess shows a small error range, lower than in Core B. Napierian logarithms have been calculated for these values and they have been represented against depth (Fig. 11). Based on the CIC model, the regression line constructed from the obtained data (-0,1763) indicates a sedimentation rate of 0.18 cm year^{-1}. This line is based on only 6 values because not all of them seem to fall on a single line. So, in order to calculate the age of any sample from -16 cm to the surface it would seem sufficient to divide the sample depth by the sedimentation rate. Consequently, the age of FAZ2 at the base is 89 years because it has been deposited since 1914. Results are reliable for this depth interval because the fit of the logarithm to depth is good.

If the CRS model is used, two different sedimentation rates are obtained. One for the most surficial interval with a higher value and the other for the remainder of the core. This model does not seem adequate as too many intermediate concentrations need to be extrapolated.

Analyte	ER-L	ER-M	AET*b*
Nap	160	2100	500
Acy	44	640	1300
Ace	16	500	150
Flu	19	540	350
Phe	240	1500	260
Ant	85	1100	300
Flr	600	5100	1000
Pyr	670	2600	1000
B[a]A	260	1600	550
Chy	380	2800	900
Be[a]P	430	1600	700
D[ah]A	63.4	260	100
Low Mol. Wt PAH	552		3160
High Mol. Wt. PAH	1700		9600
Σ*PAH*	4000	45000	22000

Table 6.- ER-L, ER-M and AET values (mg kg^{-1}) for PAHs in Core M sediment samples.

Table 6.- Valores ER-L, ER-M y AET (mg kg^{-1}) para los PAHs en las muestras sedimentarias del pequeño sondeo M.

The ^{137}Cs concentrations show small measurement errors but do not exhibit a clear evolution with depth and significant values coexist with others well below the detection limit. This may be a consequence of the radiometric measurement or the sedimentation process in this marsh area and, therefore, they have not been taken into account.

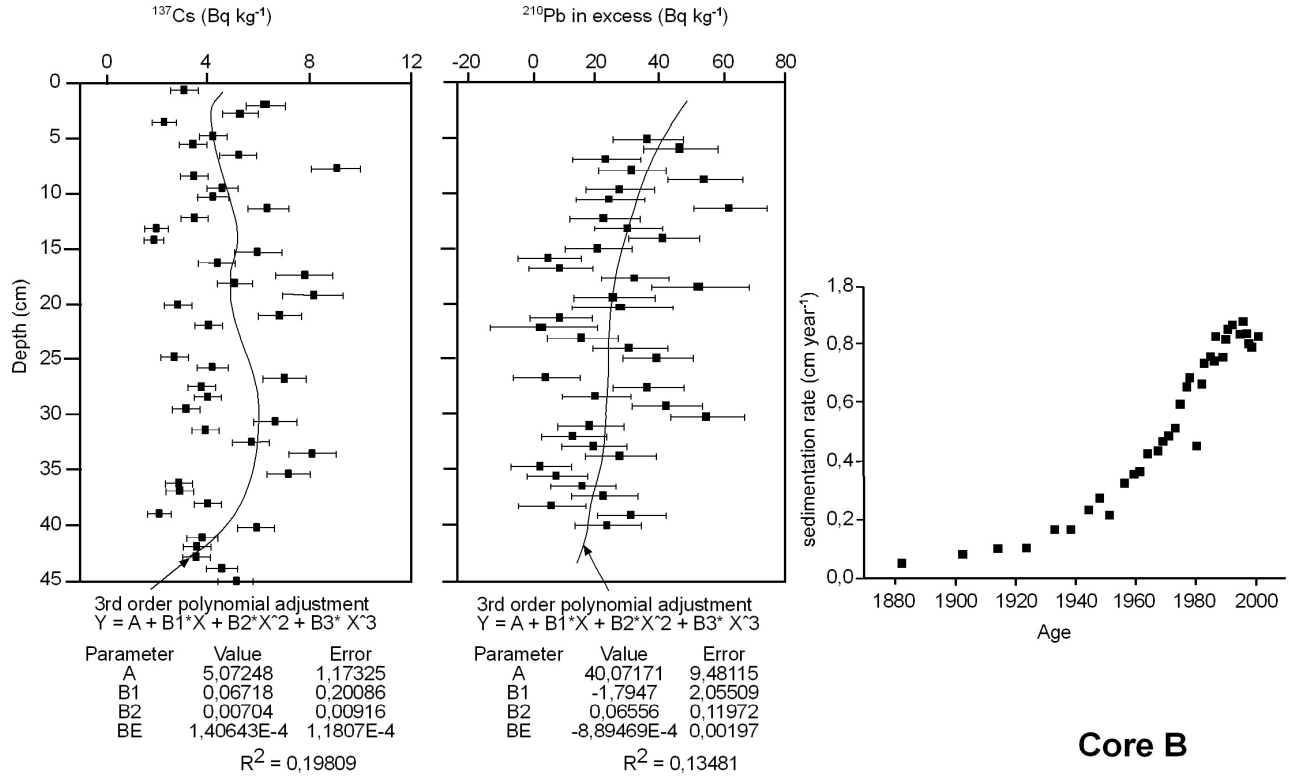

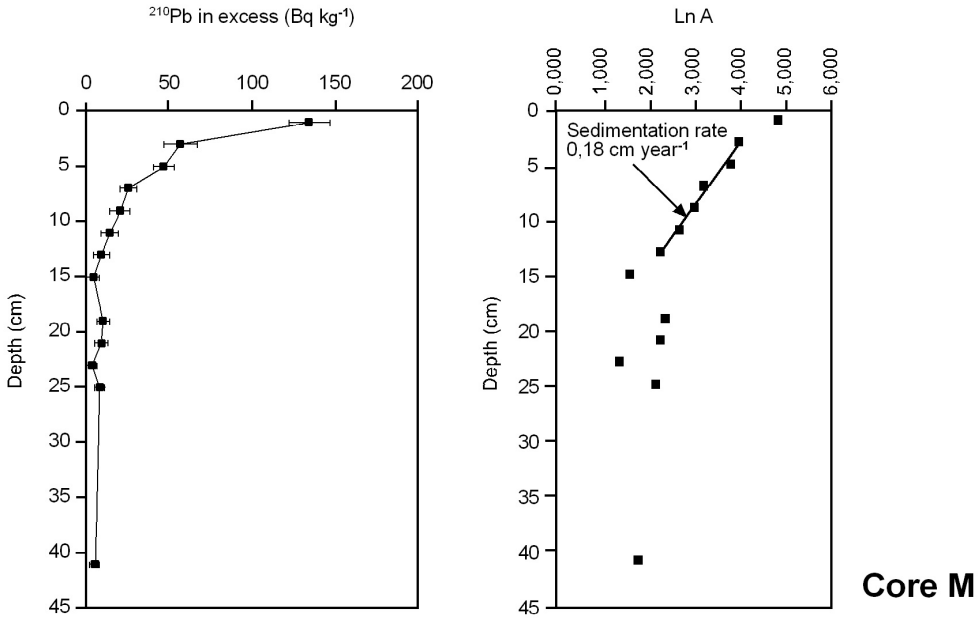

Fig. 11.- ^{137}Cs and ^{210}Pb activity (Bq kg^{-1}) with depth and sedimentation rate in core B (tidal flat) and core M (marsh) from the Muskiz estuary.
Fig. 11.- Actividad de ^{137}Cs y ^{210}Pb (Bq kg^{-1}) en función de la profundidad y la tasa de sedimentación en los pequeños sondeos B (canal principal) y M (marisma) de la Ría de Muskiz.

4.5. Interpretation of the sedimentary record

Based on ^{210}Pb radiometric dating, sediment cores from the Muskiz estuary provide information on its environmental evolution during the last 120 years.

Geochemical profiles of Core B show low metal and PAH values throughout the whole sedimentary record in contrast with results obtained from other moderately polluted nearby estuaries like Plentzia (Cearreta *et al.*, 2002) or Santander (Viguri *et al.*, 2007) where low metal

contents, characteristic of the pre-industrial time, are followed upwards by increased values associated to anthropogenic effluents during the 20th century. Enriched levels detected at 31 and 37 cm depth (Fig. 8) are considered to be the result of post-depositional modifications due to early diagenetic effects. The sediment and its microfaunal content indicates the presence of firstly a sandy intertidal flat developed under normal-salinity conditions in the middle estuary (FAZ1) which existed until 1914, then this was followed by an increase in brackish estuarine conditions (FAZ2a) until 1951 when a low marsh (FAZ2b) extended over the area during a short period of time (Fig. 6). These environments developed before the installation of the oil refinery in 1970 in the original estuarine domain. This included reconstruction of the tidal channel (Fig. 1) and excavation and dumping of sediments (FAZs 2c and 3) during this severe physical alteration. Finally, modern muddy environmental conditions (FAZ 4) have become established since 1997.

On the other hand, Core M sediments can be divided into two well defined environments. Firstly, a sandy intertidal flat under normal-salinity conditions equivalent to FAZ1 of Core B, was followed after 1914 by a vegetated marsh environment, slightly enriched in heavy metals, that continues up to the present. This enrichement is probably related to the potential capacity of vegetation to retain metals (Chenhall *et al.*, 1992; Caçador *et al.*, 1996) rather than post-depositional remobilizations as vegetation makes these marshy areas less susceptible to these processes (Cundy *et al.*, 1997).

The recent environmental evolution of the Muskiz estuary is not related to persistent historical pollution but rather to the extensive occupation of the original estuary by an oil refinery after 1970. This included modification of the original main tidal channel and an impoverishment of the general environment with the almost complete loss of the estuary and its various sub-environments.

5. Summary and conclusions

In order to identify and assess the environmental impact of the largest oil refinery in Spain, which was built on the Muskiz estuary in 1970, this study used an integrated high-resolution microfaunal-geochemical approach to differenciate between natural processes and anthropogenic impacts in this area during the last 120 years. The results obtained from the modern environments indicate that organic and inorganic pollutant contents are low and similar to those determined in sediments from other nearby, well-preserved estuaries. However, in contrast with these geochemical results, both abundance and number of species of the microfauna are very low along the estuarine intertidal flats and they have normal values on the marsh areas. The main natural environmental change recorded in the sediments of the middle estuary was around 1914 when a sandy, normal-marine environment was transformed into muddy, brackish conditions. The location of the oil refinery on the estuarine domains represents the main anthropogenic impact on this coastal area. However, there has been no persistent historical organic or inorganic pollution in this estuary since 1970, but the large area of occupation of the estuary has merely eliminated the original ecosystems and provoked a subsequent general impoverishment of its environmental quality.

Acknowledgements

We are grateful to Alejandra Fernández (Osakidetza Health Centre, Gernika) who carried out the X-radiograph of Core M. Lead-210 and Cs-137 analyses were carried out at University of Cantabria (Core B) and Univerity of Bordeaux I (Core M). Organic content analyses were performed by Neiker (Derio). Graham Evans (University of Southampton, UK), Francisco Fatela (University of Lisbon, P) and Eduardo Leorri (University of Angers, F) critically reviewed and improved greatly the original manuscript.This work was funded by Contracts 9/UPV00121.310-14452/2002 from the University of the Basque Country, UNESCO 06/08 and GIC07/32-IT-332-07 from the Basque Government. María Alday received a postgraduate grant from the Basque Government (BFI00.8.0) and this work represents part of her research leading to a PhD degree carried out in the UPV/EHU.

References

Alday, M. (2004): *Registro micropaleontológico holoceno de la transformación ambiental de origen natural y antrópico en el litoral atlántico ibérico.* Unpublished PhD Thesis, University of the Basque Country: 296 p.

Apellaniz, J.M., Nolte, E. (1967): La Necrópolis y el poblado de Ranes (Abanto y Ciérvana, Vizcaya). *Munibe*, 19: 299-314.

Bartolomé, L., Cortazar, E., Rasposo, J.C., Usobiaga, A., Zuloaga, O., Etxebarria, N., Fernández, L.A., (2005): Simultaneous microwave-assisted extraction of polycyclic aromatic hydrocarbons, polychlorinated biphenyls, phthalate esters and nonylphenols in sediments. *Journal of Chromatography A*, 1068: 229-236.

Bartolomé, L., Tueros, I., Cortazar, E., Raposo, J.C., Sanz, J., Zuloaga, O., de Diego, A., Etxebarria, N., Fernández, L.A., Madariaga, J.M. (2006): Distribution of trace organic pollutants and total mercury in sediments from the Bilbao and Urdaibai estuaries (Bay of Biscay). *Marine Pollution Bulletin*, 52: 1111-1117.

Caçador, I., Vale, C., Catarino, F. (1996): Accumulation of Zn, Pb, Cu, Cr and Ni in sediments between roots of the Tagus estuary salt marshes, Portugal. *Estuarine, Coastal and Shelf Science*, 42: 393-403.

Cearreta, A., Irabien, M.J., Leorri, E., Yusta, I., Croudace, I.W., Cundy, A.B. (2000): Record of anthropogenic impacts on the Bilbao Estuary, N. Spain: geochemical and microfaunal evidence. *Estuarine, Coastal and Shelf Science*, 50: 571-592.

Cearreta, A., Irabien, M.J., Ulibarri, I., Yusta, I., Croudace, I.W., Cundy, A. (2002): Recent salt marsh development and natural regeneration of reclaimed areas in the Plentzia estuary, N. Spain. *Estuarine, Coastal and Shelf Science*, 54: 863-886.

Cearreta, A., Murray, J.W. (2000): AMS 14C dating of Holocene estuarine deposits: consequences of high energy and reworked foraminifera. *The Holocene*, 10: 155-159.

CEDEX (1994): *Recomendaciones para la gestión del material dragado en los puertos españoles.* Ministerio de Obras Públicas, Transportes y Medio Ambiente, Madrid: 45 p.

Chenhall, B.E., Yassini, I., Jones, B.J. (1992): Heavy metal concentration in lagoonal saltmarsh species, Ilhawarra region, southern Australia. *The Science of the Total Environment*, 12: 203-225.

Cundy, A.B., Croudace, I.W. (1995): Sedimentary and geochemical variations in a salt marsh/mud flat environment from the mesotidal Hamble estuary, southern England. *Marine Chemistry*, 51: 115-132.

Cundy, A.B., Croudace, I.W., Thomson, J., Lewis, J.T. (1997): Reliability of salt marshes as "geochemical recorders" of pollution input: a case study from contrasting estuaries in southern England. *Environmental Science and Technology*, 31: 1093-1101.

Froelich, P.N., Klinkhammer, G.P., Bender, M.L., Luedtke, N.A., Heath, G.R., Cullen, D., Dauphin, P. (1979): Early oxidation of organic matter in pelagic sediments of the eastern equatorial Atlantic, suboxic diagenesis. *Geochimica et Cosmochimica Acta*, 20: 2059-2067.

García-Arberas, L. (1999): *Estudio del zoobentos intermareal de los fondos blandos de los estuarios de La Arena, Plencia y Gernika (Bizkaia)*. Servicio Editorial de la Universidad del País Vasco/EHU, Leioa: 497 p.

Gobierno Vasco (1998a): *Avance del Plan Territorial Sectorial de Zonas Húmedas de la Comunidad Autónoma del País Vasco*. Servicio de Publicaciones de la Administración de la Comunidad Autónoma del País Vasco, Vitoria-Gasteiz: 290 p.

Gobierno Vasco (1998b): *La red de vigilancia y control de la calidad de las aguas litorales del País Vasco: años 1995 y 1996*. Servicio Central de Publicaciones, Vitoria-Gasteiz. Recursos Hídricos, 29: 196 p.

Gobierno Vasco (1999): *La red de vigilancia y control de la calidad de las aguas litorales del País Vasco: años 1997 y 1998*. Servicio Central de Publicaciones, Vitoria-Gasteiz. Recursos Hídricos, 46: 92 p.

ICES (1989): *Report of the ICES Advisory Commitee on Marine Pollution*. ICES Coop. Res. Report: 167 p.

Irabien, M.J. (1993): *Caracterización mineralógica y geoquímica de los sedimentos actuales de los ríos Nervión, Butrón, Oka y Nive. Índices de gestión ambiental*. Unpublished PhD Thesis, University of the Basque Country: 320 p.

Irabien, M.J., Velasco, F. (1999): Heavy metals in the Oka river (Urdaibai National Biosphere Reserve, Northern Spain). Lithogenic and anthropogenic effects. *Environmental Geology*, 37: 54-63.

Lederer, C.M., Hollander, J.M., Perlman, I. (1967): *Table of isotopes.* Ed. Wiley and Sons, New York: 594 p.

Long, E.R., MaTDonald, D.D., Smith, S.L., Calder, F.D. (1995): Incidence of adverse biological effects within ranges of chemical concentrations in marine and estuarine sediments. *Environmental Management*, 19: 81-97.

Murray, J.W. (1979): *British Nearshore Foraminiferids*. Synopsis of the British Fauna (New Series), 16, Academic Press, London: 68 p.

Murray, J.W. (1991): Ecology and distribution of benthic foraminifera. In: Lee, J.J., Anderson, R.O. (Eds.), *Biology of Foraminifera*. Academic Press, London: 221-254

OSPAR (1998): *OSPAR guidelines for the Management of Dredged Material*. Summary Record OSPAR 98/14/1-E, Anex 43.

Quindós, L.S., Fernández, P.L., Soto, J., Ródenas, C., Gómez, J. (1994): Natural radioactivity in Spanish soils. *Health Physics*, 66: 194-200.

Rivas, V. (1991): *Evolución reciente y estado actual del litoral cantábrico oriental*. Unpublished PhD Thesis, University of Murcia, 2 volumes: 537 p.

Rogers, M.J. (1976): An evaluation of an index of affinity for comparing assemblages, in particular of foraminifera. *Palaeontology*, 19: 503-515.

Seebold, J.I. (1981): *Distribución y comportamiento de los metales pesados en los sedimentos de las rías de Vizcaya (Bilbao, Guernica y Plencia)*. Unpublished MSc Thesis, University of the Basque Country: 154 p.

Spencer, K.L., Cundy, A.B., Croudace, I.W. (2003): Heavy metal distribution and early-diagenesis in salt marsh sediments from the Medway estuary, Kent, UK. *Estuarine, Coastal and Shelf Science*, 57: 43-54.

Thomson, J., Higgs, N.C., Croudace, I.W., Colley, S., Hydes, D.J. (1993): Redox zonation of elements at an oxic/post-oxic boundary in deep-sea sediments. *Geochimica et Cosmochimica Acta*, 57: 579-595.

Thomson, J., Dyer, F.M., Croudace, I.W. (2002): Records of radionuclide deposition in two salt marshes in the United Kingdom with contrasting redox and accumulation conditions. *Geochimica et Cosmochimica Acta*, 66: 1011-1023.

Viguri**,** J.R., Irabien, M.J., Yusta, I., Soto, J., Gómez, J., Rodríguez, P., Martínez-Madrid, M., Irabien, J.A. and Coz, A. (2007): Physico-chemical and toxicological characterization of the historic estuarine sediments: a multidisciplinary approach. *Environment International,* 33: 436-444.

Wake, H. (2005): Oil refineries: a review of their ecological impacts on the aquatic environment. *Estuarine, Coastal and Shelf Science*, 62: 131-140.

Walton, W.R. (1952): Techniques for recognition of living foraminifera. *Contributions from the Cushman Foundation for Foraminiferal Research*, 3: 56-60.

Williams, T.P., Bubb, J.M., Lester, J.N. (1994): Metal accumulation within salt marsh environment: A review. *Marine Pollution Bulletin*, 28: 277-290

Yunker, M.B., MaTDonald, R.W., Vingarzan, R., Mitchell, R.H., Goyette, D., Sylvestre, S. (2002): PAHs in the Fraser River basin: a critical appraisal of PAH ratios as indicators of PAH source and composition. *Organic Geochemistry*, 33: 489-515.

Zapata, L. (Coor.) (1995): El depósito sepulcral calcolítico de la cueva de Pico Ramos (Muskiz, Bizkaia). *Munibe*, 47: 33-197.

Zwolsman, J.J.G., Berger, G.W., van Eck, G.T.M. (1993): Sediment accumulation rates, historical input, post-depositional mobility and retention of major elements and trace elements in salt marsh sediments of the Scheldt estuary, SW Netherlands. *Marine Chemistry*, 44: 73-94.

Appendix 1.- Faunal reference list. TL: intertidal flat living; TD: intertidal flat dead; B: intertidal flat core; ML: marsh living; MD: marsh dead; M: marsh core.

Acervulina inhaerens Schultze, 1854 (B, M)
Adelosina cliarensis (Heron-Allen and Earland) = *Miliolina cliarensis* Heron-Allen and Earland, 1930 (TL, TD, B, MD, M)
Adelosina striata d'Orbigny, 1826 (TL, B, MD, M)
Ammonia tepida (Cushman) = *Rotalia beccarii* (Linné) var. *tepida*, 1926 (TL, TD, B, ML, MD, M)
Astacolus crepidulus (Fichtel and Moll) = *Nautilus crepidula* Fichtel and Moll, 1798 (B, MD, M)
Asterigerinata mamilla (Williamson) = *Rotalia mamilla* Williamson, 1858 (TL, TD, B, MD, M)
Aubignyna hamblensis Murray, Whittaker and Alve, 2000 (TL, TD, B)
Brizalina britannica (Macfadyen) = *Textularia variabilis* Williamson var. *laevigata* Williamson, 1858 (TL,TD,B, ML, MD, M)
Brizalina difformis (Williamson) = *Textularia variabilis* Williamson var. *difformis* Williamson, 1858 (TD, B, MD)
Brizalina spathulata (Williamson) = *Textularia variabilis* Williamson var. *spathulata* Williamson, 1858 (TL, TD, B, MD)
Brizalina variabilis (Williamson) = *Textularia variabilis* Williamson, 1858 (TD, B, MD)
Bulimina elongata d'Orbigny, 1846 (MD, M)
Bulimina gibba Fornasini, 1902 (TL, TD, B, ML, MD, M)
Bulimina marginata d'Orbigny, 1826 (TD, B, MD)
Buliminella elegantissima (d'Orbigny) = *Bulimina elegantissima* d'Orbigny, 1839 (TD, B)
Cassidulina carinata (Silvestri) = *Cassidulina laevigata* d'Orbigny var. *carinata* Silvestri, 1896 (M)
Cassidulina obtusa Williamson, 1858 (TD, B, MD, M)
Cibicides lobatulus (Walker and Jacob) = *Nautilus lobatulus* Walker and Jacob, 1798 (TL, TD, B, ML, MD, M)
Cribroelphidium excavatum (Terquem) = *Polystomella excavata* Terquem, 1875 (TL, TD, ML, MD)
Cribroelphidium gerthi Van Voorthuysen, 1975 (B, MD, M)
Cribroelphidium oceanensis (d'Orbigny) = *Polystomella oceanensis* d'Orbigny, 1826 (TL, TD, B, ML, MD, M)
Cribroelphidium williamsoni Haynes, 1973 (TL, TD, B, ML, MD, M)
Cribrostomoides jeffreysii (Williamson) = *Nonionina jeffreysii* Williamson, 1858 (B, MD)
Eggerelloides scaber (Williamson) = *Bulimina scabra* Williamson, 1858 (B)
Elphidium crispum (Linné) = *Nautilus crispus* Linné, 1798 (TL, TD, B, MD, M)
Elphidium macellum (Fichtel and Moll) = *Nautilus macellum* Fichtel and Moll, 1798 (TD, B, MD)
Elphidium margaritaceum Cushman, 1930 (TD, B, MD, M)
Fissurina lucida (Williamson) = *Entosolenia marginata* (Montagu) var. *lucida* Williamson, 1848 (MD)
Fissurina marginata (Montagu) = *Vermiculum marginatum* Montagu, 1803 (TL, TD, B, MD)

Gaudryina rudis Wright, 1900 (B, M)
Gavelinopsis praegeri (Heron-Allen and Earland) = *Discorbina praegeri* Heron-Allen and Earland, 1913 (TL, TD, B, MD, M)
Globulina gibba (d'Orbigny) = *Polymorphina gibba* d'Orbigny, 1826 (TD, B, MD, M)
Haynesina depressula (Walker and Jacob) = *Nautilus depressulus* Walker and Jacob, 1798 (TD, B, MD, M)
Haynesina germanica (Ehrenberg) = *Nonium germanicum* Ehrenberg, 1840 (TL, TD, B, ML, MD, M)
Jadammina macrescens (Brady) = *Trochammina inflata* (Montagu) var. *macrescens* Brady, 1870 (TL, TD, B, ML, MD, M)
Lagena clavata (d'Orbigny) = *Oolina clavata* d'Orbigny, 1846 (TD, MD)
Lagena interrupta (Williamson) = *Lagena striata* (Montagu) var. *interrupta* Williamson, 1858 (B)
Lagena sulcata (Walker and Jacob) = *Serpula sulcata* Walker and Jacob, 1798 (TD, MD)
Lagena tenuis (Bornemann) = *Ovulina tenuis* Bornemann, 1855 (TD)
Lenticulina inortatus (d'Orbigny) = *Robulina inortata* d'Orbigny, 1846 (TD, B, MD, M)
Lepidodeuterammina ochracea (Williamson) = *Rotalia ochracea* Williamson 1858 (MD)
Massilina secans (d'Orbigny) = *Quinqueloculina secans* d'Orbigny, 1826 (TL, TD, B, ML, MD, M)
Miliammina fusca (Brady) = *Quinqueloculina fusca* Brady, 1870 (TL, TD, B, ML, MD)
Miliolinella subrotunda (Montagu) = *Vermiculum subrotundum* Montagu, 1803 (TL, TD, B, ML, MD, M)
Nonionella atlantica Cushman, 1947 (TD, B, MD, M)
Oolina hexagona (Williamson) = *Entosolenia squamosa* (Montagu) var. *hexagona* Williamson, 1858 (TL, TD, B, MD)
Oolina squamosa (Montagu) = *Vermiculum squamosa* Montagu, 1803 (B)
Patellina corrugata Williamson, 1858 (TD, B, MD, M)
Pateoris hauerinoides (Rhumbler) = *Quinqueloculina subrotunda* (Montagu)
forma *hauerinoides* Rhumbler, 1936 (TL, TD, B, MD, M)
Planorbulina mediterranensis d'Orbigny, 1826 (TL, TD, B, ML, MD, M)
Pyrgo depressa (d'Orbigny) = *Biloculina depressa* d'Orbigny, 1826 (B)
Quinqueloculina bicornis (Walker and Jacob) = *Serpula bicornis* Walker and Jacob, 1798 (TD, B, MD, M)
Quinqueloculina dimidiata Terquem, 1876 (B, MD)
Quinqueloculina lata Terquem, 1876 (TL, TD, B, ML, MD, M)
Quinqueloculina oblonga (Montagu) = *Vermiculum oblongum* Montagu, 1803 (TL, TD, B, MD, M)
Quinqueloculina quadrata Nörvang, 1945 (TD, B, MD, M)
Quinqueloculina seminula (Linné) = *Serpula seminulum* Linné, 1758 (TL, TD, B, ML, MD, M)
Quinqueloculina sp.1 (TD, B, MD)
Rosalina anomala Terquem, 1875 (TL, TD, B, ML, MD, M)
Rosalina irregularis (Rhumbler) = *Discorbina irregularis* Rhumbler, 1906 (TL, TD, B, ML, MD, M)
Spirillina vivipara Ehrenberg, 1843 (TL, B, MD, M)
Spiroloculina excavata d'Orbigny, 1846 (TD, B, MD, M)
Spirorutilis wrightii (Silvestri) = *Spiroplecta wrightii* Silvestri, 1903 (TD, B, MD, M)
Stainforthia fusiformis (Williamson) = *Bulimina pupoides* d'Orbigny var. *fusiformis* Williamson, 1858 (TD)
Textularia bocki Höglund, 1947 (TD, B, MD, M)
Textularia earlandi Parker, 1952 (TD, B)
Textularia saggitula Defrance, 1824 (TD, B, MD, M)
Trifarina angulosa (Williamson) = *Uvigerina angulosa* Williamson, 1858 (TD, M)
Triloculina bermudezi Acosta, 1940 (TD, B, MD, M)
Triloculina trigonula (Lamarck) = *Miliolites trigonula* Lamarck, 1804 (TD, B, MD, M)
Trochammina inflata (Montagu) = *Nautilus inflatus* Montagu, 1808 (TL, TD, B, ML, MD, M)